minerals

Review

Tectonic Evolution of the JLJB, North China Craton, Revisited: Constraints from Metamorphism, Geochemistry and Geochronology of the Ji'an Group and Related Granites

Erlin Zhu [1], Chenyue Liang [1,2,*], Changqing Zheng [1,2], Xuechun Xu [1,2] and Yan Yang [1]

[1] College of Earth Sciences, Jilin University, Changchun 130061, China
[2] Key Laboratory of Mineral Resources Evaluation in Northeast Asia, Ministry of Natural Resources, Changchun 130061, China
* Correspondence: chenyueliang@jlu.edu.cn; Tel.: +86-1516-4362-972

Abstract: The Jiao-Liao-Ji Belt (JLJB) is the most representative Paleoproterozoic orogenic belt in the North China Craton (NCC). The sedimentation, metamorphism and magmatism of the Ji'an Group and associated granites provide significant insights into the tectonic evolution of the JLJB. In this study, we have synthesized published geochemistry and geochronology data on metasedimentary, metavolcanic and igneous rocks. According to the available data, the protoliths of the metasedimentary rocks are sets of shale, wacke, arkose, quartz sandstone and carbonate, while the protoliths of the metavolcanic rocks are calc-alkaline basalt, basaltic andesite, andesite, dacite and rhyolite. The rock assemblages indicate a transformation of the tectonic environment from a passive margin to an active continental margin following the onset of plate convergence and subduction. The A2-type gneissic granite (Qianzhuogou pluton) is formed in a subsequent back-arc basin extension setting at 2.20–2.14 Ga. The Ji'an Group was finally deposited in an active continental margin during the closure of a back-arc basin at 2.14–2.0 Ga. Then, the sediments were involved in a continent–arc–continent collision between the Longgang and Nangrim blocks at ~1.95 Ga. This process was accompanied by HP granulite-facies metamorphism at ~1.90 Ga. The subsequent exhumation and regional extension resulted in decompression melting during 1.90–1.86 Ga, producing metamorphism with an isothermal decompression clockwise P–T path. The resulting metapelites are characterized by perthite + sillimanite, and mafic granulites are characterized by orthopyroxene + clinopyroxene. The S-type porphyritic granite (Shuangcha pluton) is formed during the crustal anatexis. Meanwhile, extensive anatexis produced significant heating and triggered prograde to peak metamorphism with an anticlockwise P–T path. Cordierite-bearing symplectites around the garnet in the metapelites indicate a superposed isobaric cooling metamorphism. The ages of monazites and anatectic zircons suggest that the post-exhumation cooling occurred at 1.86–1.80 Ga. The Paleoproterozoic magmatism, sedimentation and metamorphism suggest a process of subduction back-arc basin extension and closure, collision and exhumation for the tectonic evolution of the JLJB.

Keywords: Ji'an Group; geochronology; magmatism; metamorphism; Jiao-Liao-Ji Belt

check for updates

Citation: Zhu, E.; Liang, C.; Zheng, C.; Xu, X.; Yang, Y. Tectonic Evolution of the JLJB, North China Craton, Revisited: Constraints from Metamorphism, Geochemistry and Geochronology of the Ji'an Group and Related Granites. *Minerals* **2023**, *13*, 835. https://doi.org/10.3390/min13070835

Academic Editors: George M. Gibson, Jianxin Zhang and Shengyao Yu

Received: 26 February 2023
Revised: 13 June 2023
Accepted: 14 June 2023
Published: 21 June 2023

1. Introduction

The supercontinent cycle of continental assembly and breakup plays a crucial role in governing mantle dynamics and crustal growth. The Columbia/Nuna, which formed in the Paleoproterozoic, is one of the oldest supercontinents. Orogens from 2.1 to 1.8 Ga have been recognized on almost all continents, including the Transamazonian Orogen of South America, the Eburnean Orogen of West Africa, the Capricorn Orogen of Western Australia, the Transantarctic Mountains Orogen of Antarctica, the Trans-North China Orogen in North China, etc. [1–3]. As one of the oldest existing cratons, the North China Craton (NCC) records multiple tectonic, magmatic and metamorphic events [4–7]. Since the discovery of 3.8 billion-year-old rocks in the craton [8], the NCC has been the focus of extensive research.

An intensive study of the ancient orogenic belt (Neo-Archean–Paleoproterozoic) within the NCC is of great significance for elucidating the breakup and assembly of the continent [9,10]. The Jiao-Liao-Ji Belt (JLJB) is one of the most representative Paleoproterozoic orogenic belts in the NCC. While it is widely accepted that the JLJB was formed by the collision between the Longgang and Nangrim blocks, ongoing debates exist about the belt's tectonic nature (rift versus collision models; e.g., [6,11,12]). A comprehensive understanding of the Paleoproterozoic sedimentation, metamorphism and magmatism is key to resolving this controversy [9,13–20]. The widely exposed meta-igneous and metasedimentary rocks (schist, gneiss, marble, felsic gneiss, granulite and amphibolite) of the Ji'an Group, as well as the related voluminous granites (gneissic granite and porphyritic granite), provide evidence of multiple metamorphic–deformational and magmatic–tectonic events, which could serve as strong constraints on the tectonic evolution of the JLJB.

In this study, we summarize the geochemical and geochronological data of the metasedimentary and meta-igneous rocks in the Ji'an Group, as well as associated granites (sample details are listed in Appendix A). The analytical results allow us to discuss the source property, protolith, stratigraphy, petrogenesis, metamorphic evolution, nature of the magma and geochronology outline of the JLJB. After reviewing the current state of research, we propose a complete tectonic cycle, including subduction, back-arc extension, the closure of the back-arc basin, collision, post-collisional extension and exhumation, which may provide crucial insights into unraveling the evolution of the JLJB.

2. Geological Background

The NCC can be subdivided into the Western Block and the Eastern Block, as well as three Paleoproterozoic orogenic belts known as the Jiao-Liao-Ji Belt, the Trans-North China Orogen belt and the Khondalite belt [5,7]. The JLJB is located between the Nangrim and Longgang blocks in the eastern NCC (Figure 1) [11]. It consists mainly of metasedimentary rocks, meta-igneous successions and igneous rocks, including Archean–Paleoproterozoic TTG gneisses, greenschist–amphibolite–granulite facies metasedimentary rocks, various granites (gneissic granite, alkaline granite, calc-alkaline granite, porphyritic granite, etc.), bimodal volcanic rocks, mafic dykes (veins) and andesitic–rhyolitic tuffs [9,21–23]. The metasedimentary and meta-igneous successions consist of the Ji'an Group and Laoling Group in southern Jilin, the North Liaohe Group and South Liaohe Group in eastern Liaoning, the Jingshan Group and Fenzishan Group in eastern Shandong, and the Wuhe Group and Fengyang Group in Anhui Province (Figure 1b; [6,10]). Some scientists argue for an intracontinental rift model for the evolution of the JLJB based on the occurrence of bimodal volcanic rocks and A-type granites, coupled with the anticlockwise P–T paths [24–26], while others suggest a continent–arc or continent–continent collision model based on the occurrence of 2.2–2.1 Ga mafic–felsic intrusions and clockwise P–T paths of Paleoproterozoic metamorphism [27,28]. Recent studies have provided two more compelling models involving a rift–subduction–collision cycle [10,12,29,30] and a back-arc basin or retro-arc foreland basin setting [9,31,32].

The Ji'an Group, distributed in the northeast of the Paleoproterozoic JLJB, is mainly exposed in Tonghua, Jilin Province (Figure 2). It is mainly composed of aluminous schist, pelitic gneiss, felsic gneiss, granulite, interlayered marble and thin-bedded quartzite [11]. Regionally, it can be compared with the South Liaohe Group, Jingshan Group and Motianling Group. The Ji'an Group is divided into Mayihe, Huangchagou and Dadongcha formations from the bottom upwards (Figure 3). The sediments are considered to have been deposited in an active continental margin environment at 2.2–1.9 Ga [33–35] and generally experienced greenschist to low-amphibolite facies metamorphism, with some parts of the sequence attaining high-amphibolite to granulite facies [11,35–37].

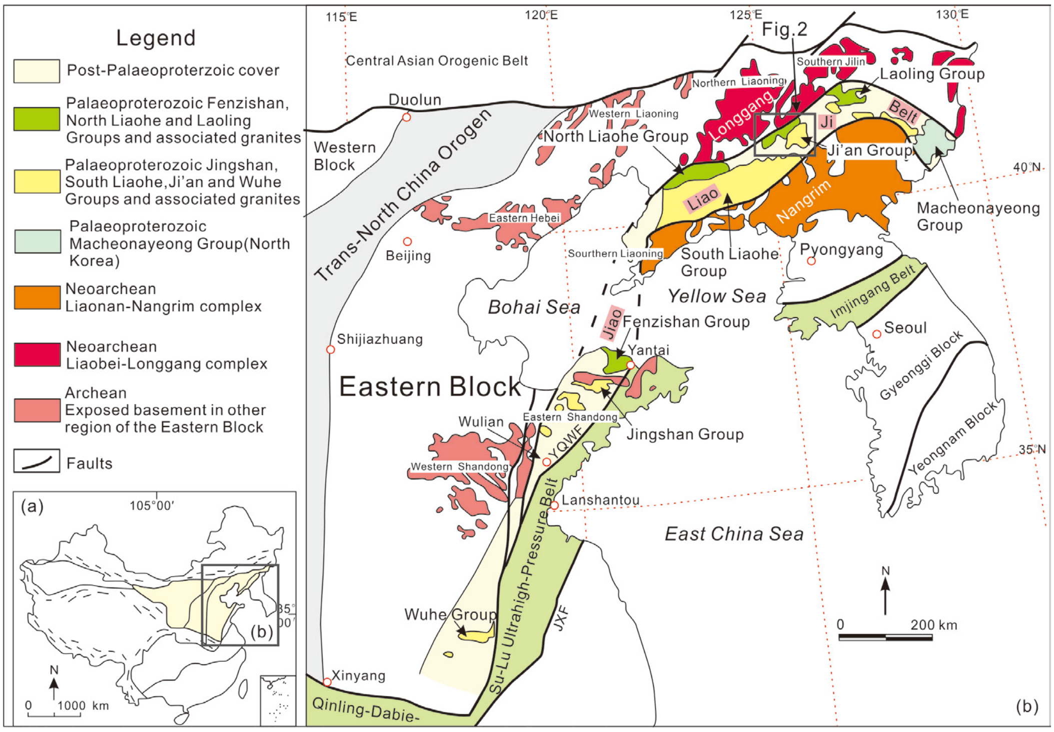

Figure 1. Simplified geological maps of the North China Craton (NCC) and the Jiao-Liao-Ji Belt (JLJB). (**a**) Tectonic setting of the NCC; (**b**) regional Precambrian geological map of the Eastern Block in the NCC (modified after [6]).

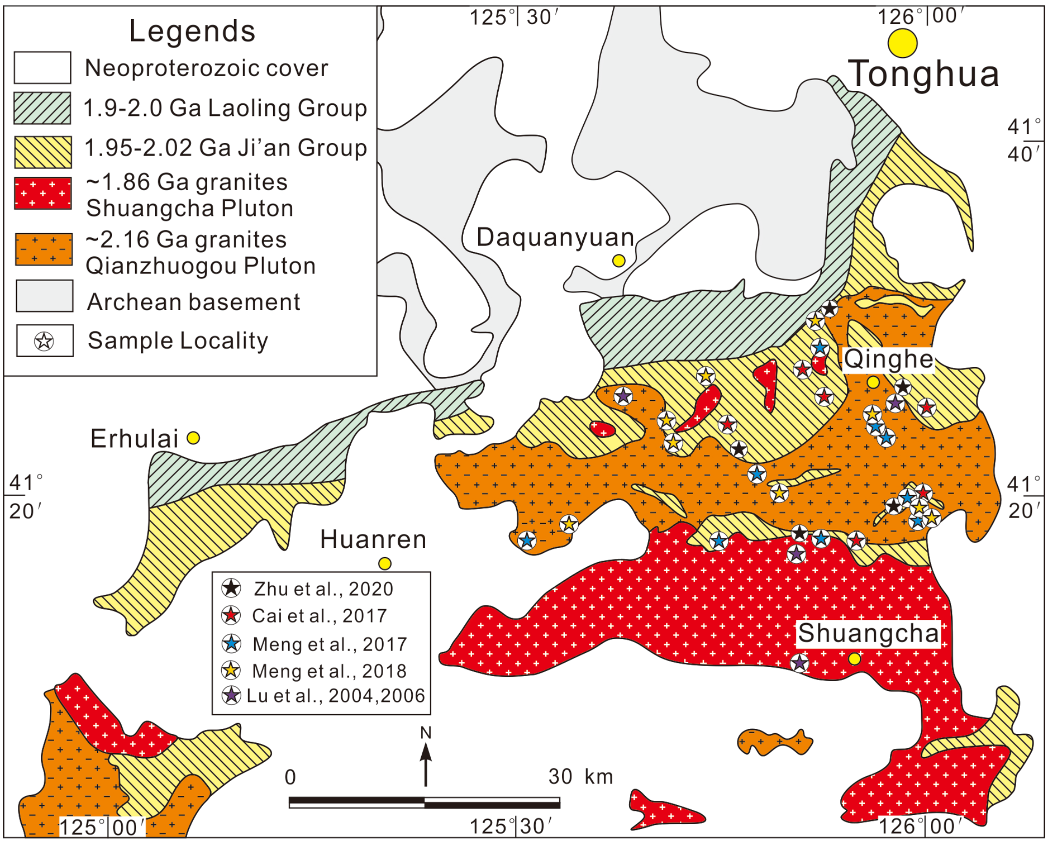

Figure 2. Distribution of the Paleoproterozoic Ji'an Group and Laoling Group and associated granites in the Tonghua area (modified after [22]).

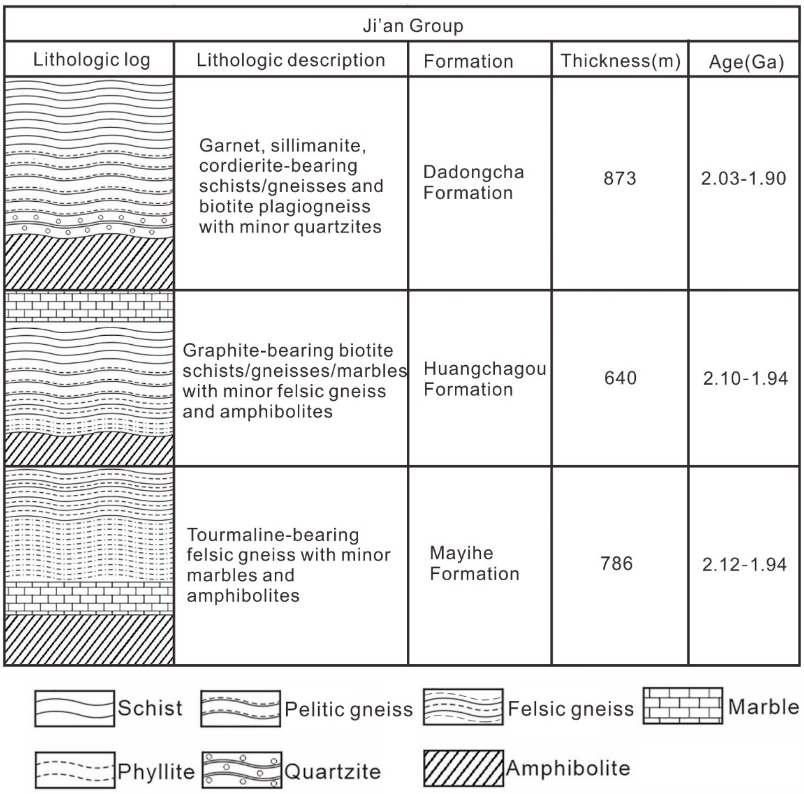

Figure 3. Lithostratigraphic units of the Ji'an Group (modified after [33]).

The Mayihe Formation is characterized by boron-bearing felsic gneisses and is mainly distributed in Jiayichuan, Huadianzi, Minshan and Wenzigou in the Ji'an area. The lower section of the formation is characterized by amphibolites and felsic gneisses. The middle section consists of serpentinized, dolomitic marbles and a few felsic gneisses and amphibolites. The upper section is dominated by tourmaline-bearing felsic gneisses, tourmaline-bearing quartzites and mica schists (Figure 3).

The Huangchagou Formation is characterized by graphitic rocks and is mainly distributed in Sanbanjiang, Quanyangou, Yaoyingzi, Toudao, Qinghe and Wenzigou in the Tonghua area. The lower section is characterized by graphitic felsic gneisses, interlayered graphitic garnet–biotite schist-gneisses, amphibolites, etc. The middle section is dominated by amphibolites, interlayered graphitic felsic gneisses, graphitic mica schist-gneisses and graphitic marbles. The upper section is mainly composed of graphitic felsic gneisses, graphitic marbles, interlayered graphite-mica schists, graphitic calcium–magnesium silicate rocks, mica schists and amphibolites.

The Dadongcha Formation is characterized by aluminum-bearing gneisses and is mainly distributed in the towns of Toudao and Qinghe. The lower section is characterized by garnet felsic gneisses, interlayered quartzites, garnet–mica schists and garnet–sillimanite–plagioclase gneisses. The upper section is dominated by garnet–sillimanite–plagioclase gneisses, garnet–cordierite–plagioclase gneisses and interlayered felsic gneisses.

In addition, voluminous Palaeoproterozoic igneous rocks are associated with the metasedimentary and meta-igneous successions in the Ji'an Group, mainly including the Qianzhuogou pluton and Shuangcha pluton [38]. The Qianzhuogou pluton is mostly in contact with the Huangchagou Formation. It is mainly composed of gneissic monzonitic granite and syenogranite and displays geochemical signatures of A2-type granite [38]. The deformed A2-type granite of 2.2–2.1 Ga is usually interpreted as being emplaced during an oceanic plate subduction environment [28,39]. The Shuangcha pluton mostly intruded into the Dadongcha Formation. It is characterized by abundant potassium feldspar and garnet phenocrysts and is known as porphyritic granite. The undeformed porphyritic granite was predominantly emplaced at ca. 1.88–1.85 Ga, suggesting a post-collisional or post-orogenic extensional setting [38,39].

3. Representative Petrography and Microstructures

The greenschist–amphibolite–granulite facies metasedimentary and meta-igneous successions are widespread in the Ji'an Group. Within these successions, the pelitic garnet–sillimanite–cordierite–biotite gneisses and mafic clinopyroxene–orthopyroxene granulites preserve mineral assemblages consistent with granulite-facies metamorphism. The garnet–sillimanite–cordierite–biotite gneisses consist mainly of garnet (10%–15%), plagioclase (10%–15%), potassium feldspar (15%–25%), quartz (15%–20%), cordierite (20–25%), biotite (8%–10%), sillimanite (5%–8%) and small amounts of magnetite and ilmenite (1%–2%). Most garnet porphyroblasts are sieve-shaped, elongated or rounded, with a grain size of about 0.5–4 mm. Fibrous sillimanite, fine-grained biotite, quartz and ilmenite/magnetite inclusions can be found in garnet. In the matrix, acicular sillimanite, biotite, potassium feldspar and plagioclase are arranged discontinuously forming a gneissic structure. Symplectic cordierites form rims around the garnets (Figure 4c–f). The Cpx-Opx granulite is characterized by a mineral assemblage of coarse-grained clinopyroxene, orthopyroxene, garnet, amphibole, biotite, plagioclase and quartz. Clinopyroxene is dominated by diopside. Amphiboles form rims around the clinopyroxene. Inclusions of biotite grains can be observed within the clinopyroxene [37]. In addition, field observations show that felsic melts of varying sizes, irregular veinlets, reticulate veins and lenses of group distribution in the metapelites are associated with anatexis (Figure 4a,b).

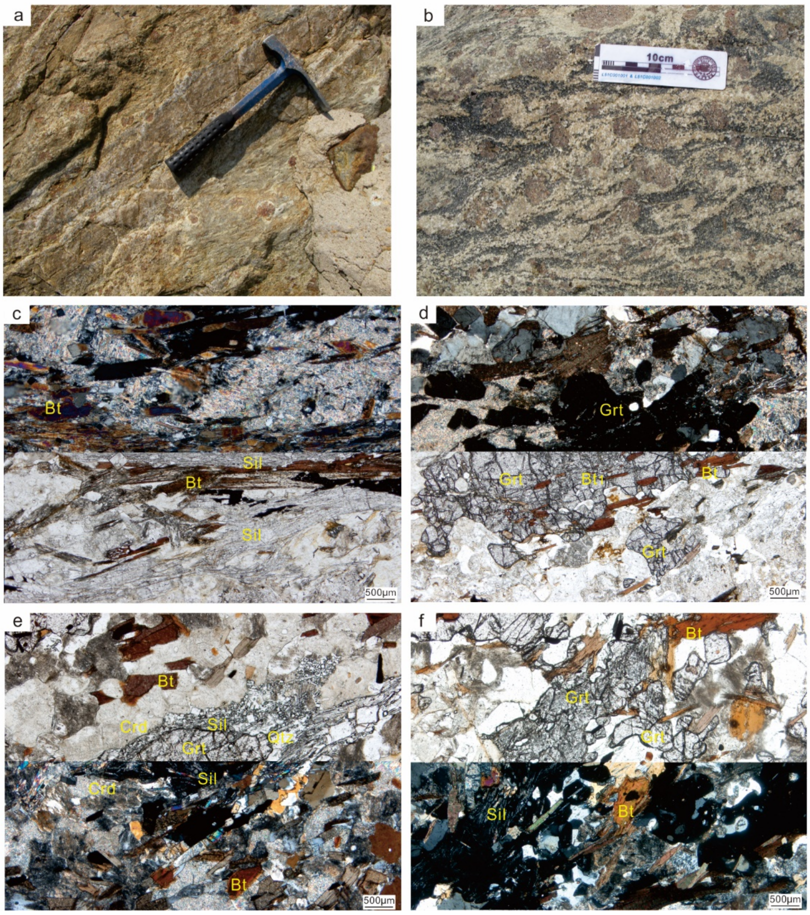

Figure 4. Representative field photographs and photomicrographs of the metapelites. (**a**,**b**) Garnet–sillimanite–cordierite–biotite gneiss; (**c**–**f**) elongated porphyroblastic garnet associated with matrix sillimanite, biotite, feldspar and quartz. The fibrous sillimanite is enclosed in garnet, and degenerative cordierite appears in the matrix. Data from [35].

4. Metamorphic Evolution of the Ji'an Group

The metamorphic evolution of the JLJB is now reasonably well known. Previous investigations have shown that the the Jingshan, Fenzishan and Wuhe Groups in the Jiaobei area underwent granulite-facies metamorphism. In contrast, the metamorphism of the Liaohe and Ji'an Groups in the Liaoji area only reached greenschist–amphibolite facies [11,22]. However, in recent years, granulite facies mafic rocks and metapelites have been identified in the Ji'an Group [37] and the South Liaohe Group [17].

The process of metamorphism can be divided into three stages: prograde, peak and retrograde. The mineral assemblages and the metamorphic reactions differ in each stage, but the prograde reactions are often overprinted by the retrograde reactions. Based on the petrography, mineral chemistry and phase equilibria modeling, we present a careful review of the metamorphic evolution of the felsic–mafic granulites in the Ji'an Group [36,37].

4.1. Peak Stage

The Cpx-Opx mafic granulite is characterized by a mineral assemblage of coarse-grained clinopyroxene, orthopyroxene, garnet, amphibole, biotite, plagioclase and quartz. Possible reactions include the following: Hb + Pl $\rightarrow$ Cpx + Opx + Hb + Pl + H_2O; Hb + Qtz $\rightarrow$ Cpx + Opx + Pl + H_2O; Opx + Pl $\rightarrow$ Cpx + Grt + Qtz.

The metapelite is characterized by a mineral assemblage of sillimanite, biotite, plagioclase, K-feldspar, perthite, quartz and garnet. The garnet rims are replaced by large biotite, potassium feldspar, sillimanite and quartz grains. Garnet may grow continuously via the consumption of sillimanite and biotite. Possible reactions include the following: Bt + Sil + Qtz $\pm$ Pl$\rightarrow$Grt $\pm$ Kfs $\pm$ Melt [40]; Bt + Pl + Qz $\rightarrow$ Grt + Melt [41].

4.2. Retrograde Stage

The Cpx-Opx mafic granulite is characterized by a mineral assemblage of orthopyroxene, clinopyroxene, biotite, plagioclase and quartz. The coarse-grained orthopyroxene is present in the garnet relict. The possible reactions include the following: Grt + Qz $\rightarrow$ Opx + Pl [41]; Bt + Pl + Qz $\rightarrow$ Opx + Grt + Melt.

The metapelites are characterized by a mineral assemblage of cordierite, sillimanite, biotite, plagioclase, quartz and garnet (rim). Garnets are rimmed by the coarse-grained cordierite and a symplectic texture (cordierite + sillimanite + quartz). Possible reactions include the following: Grt + Sil + Qz $\rightarrow$ Crd; Grt + Sil + Melt $\rightarrow$ Crd + Bt + Fe-Oxide.

4.3. P–T Paths

Systematic petrographic observations, geothermobarometry (Grt-Bt and Grt-Crd) and pseudosection thermobarometry (Thermocalc and Perplex) have been used to estimate the P–T conditions of different metamorphic stages of the Ji'an Group. Conventional geothermobarometry suggests that the P–T condition of the garnet–cordierite–biotite gneiss is ~750–700 °C and ~0. 65–0.52 GPa, which was previously attributed to amphibolite facies metamorphism with anticlockwise P–T paths [24]. However, recent phase equilibria models of some metapelites in the Ji'an Group limit the the P–T conditions of the peak stages to ~1.0–0.7 GPa/890–820 °C and the retrograde stages to ~0.7–0.5 GPa/760–620 °C, which have been attributed to granulite facies metamorphism with clockwise P–T paths (Figure 5, [18,35–37]).

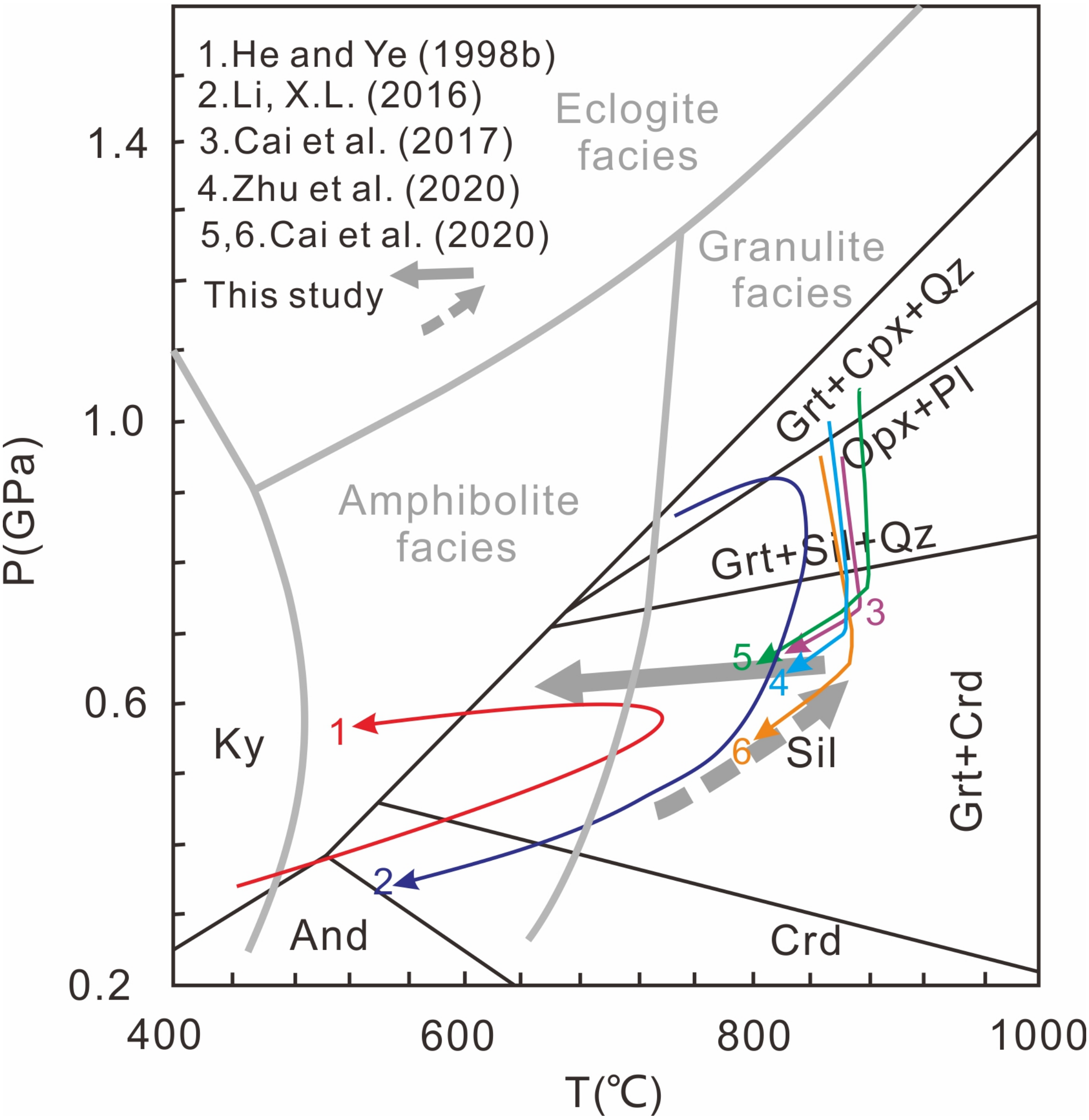

Figure 5. Metamorphic P–T paths for the Ji'an Group. Data from [24,35–37,42].

5. Geochemistry of the Ji'an Group

5.1. Meta-Igneous Rocks

A large number of meta-igneous rocks are found in the lower section of the Ji'an Group, including pyroxene amphibolites, amphibole–plagioclase gneisses, biotite–plagioclase gneisses and felsic gneisses (Figure 6a) [43]. They display medium- to fine-grained granoblastic textures with subhedral–anhedral pyroxene, biotite and feldspar. Considering that the samples may have undergone dehydration and metamorphism, the mobile components cannot be used to determine the properties of the original rocks. The Nb/Y–Zr/TiO_2*0.0001 diagram is effective in evaluating the original properties of the meta-igneous rocks. As shown in Figure 6b, the protoliths of the meta-igneous rocks consist mainly of calc-alkaline basalt, basaltic andesite, andesite, dacite and rhyolites.

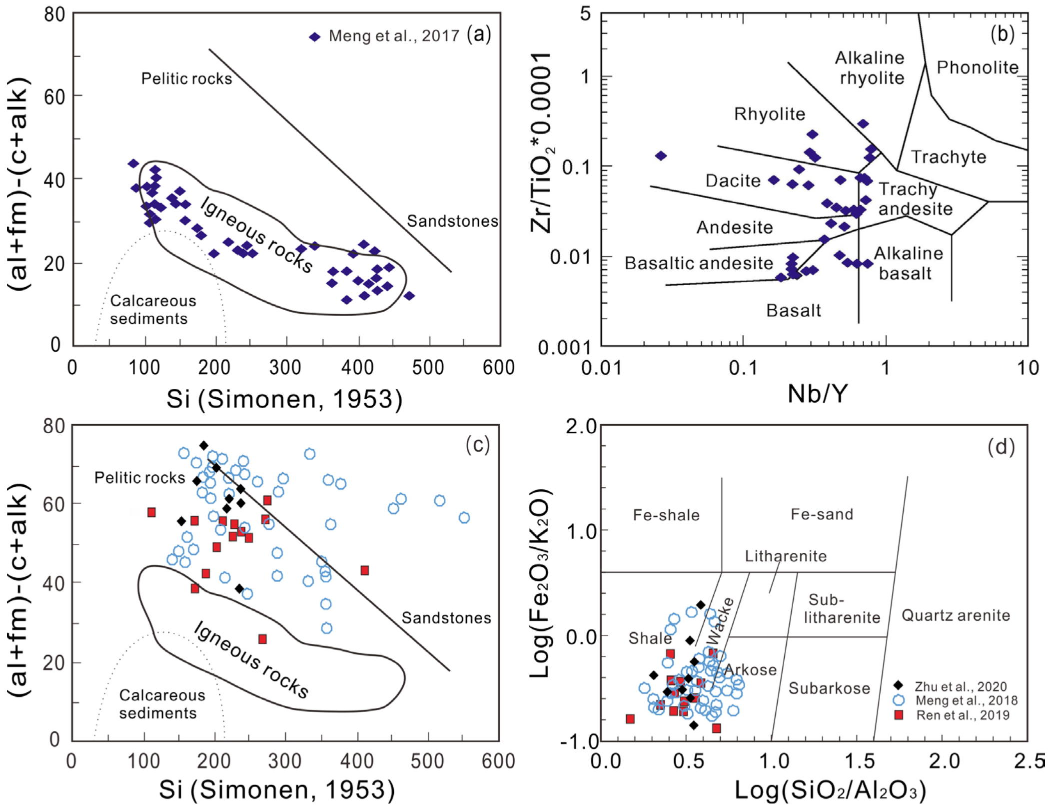

Figure 6. Classification diagrams for the metasedimentary and metavolcanic rocks. (**a**,**c**) (al + fm) − (c + alk) − Si, al = [Al_2O_3], fm = [FeO] + 2[Fe_2O_3] + [MnO] + [MgO], c = [CaO], alk = [K_2O] + [Na_2O] [44]; (**b**) Nb/Y versus Zr/TiO_2*0.0001; (**d**) log (Fe_2O_3/K_2O) versus log (SiO_2/Al_2O_3) [45]. Data sources: [33,35,38,43,46].

5.2. Metasedimentary Rocks

The Ji'an Group is characterized by thick successions of metasedimentary rocks, including aluminous schist, pelitic gneiss, felsic gneiss, granulite, interlayered marble and thin-bedded quartzite. The metasedimentary rocks of the Ji'an Group are generally enriched in Al_2O_3, depleted in CaO and FeO_T, have K_2O/Na_2O values of >1 and contain garnet and cordierite, all of which are consistent with a metasedimentary origin. The chemical composition of sedimentary rocks depends on the composition of its source rocks. Here, we reconstruct the source properties by some specific discrimination diagrams [47] based on the geochemical data in the literature [33,35,46]. In the (al + fm)–(c + alk) diagram (Figure 6c), the data fall in the area of the pelitic sedimentary rocks. Combined with the sediment assemblage and information from the log (Fe_2O_3/K_2O)–log (SiO_2/Al_2O_3) diagram (Figure 6d), the protoliths of metasedimentary rocks are mainly shale, wacke, arkose, quartz sandstone and carbonate.

6. Geochronology of the Ji'an Group and Related Granites

The Paleoproterozoic JLJB has a complex origin and underwent multistage evolution. The geochronology of the metasedimentary rocks and related granites can provide significant constraints on the formation of the JLJB. Based on the published zircon isotope geochronology data, zircon trace element data (e.g., Th and U) and the geochronological outline of the metamorphism and magmatism in the Ji'an Group [9,34,35,38,43,48], we provide constraints in the petrogenic age of the protoliths (detrital zircons with Th/U > 0.4), the metamorphic age of the metasedimentary rocks (metamorphic zircons with Th/U < 0.1) and the Paleoproterozoic magmatism (magmatic zircons with Th/U > 0.4). The metamorphic zircons in the Ji'an Group suggest that the metamorphism can be divided into two periods of 1950–1870 Ma and 1870–1800 Ma, with peak ages of 1901 Ma and 1860 Ma, respectively (Figure 7c). The ages of metamorphic zircons are consistent with the metamorphic events at 1.90 and 1.85 Ga suggested by Meng et al. [43]. Additionally, the younger ages down to 1800 Ma may indicate a cooling stage. The detrital zircons in the Ji'an Group show four statistical ages of 2191–2138, 2120–2084, 2048–1995 and 1887–1852 Ma, with peak ages of 2670 and 2460 Ma (Figure 7d). These data suggest four periods of magmatism in the Paleoproterozoic JLJB. The magmatic zircons of the porphyritic granite (Shuangcha pluton) are mainly concentrated in 1887–1852 Ma with ages of ~2175 Ma and ~2625 Ma. The magmatic zircons of the gneissic granite (Qianzhuogou pluton) yield ages of 2200–1800 Ma with peaks at 2191–2138 Ma. Consequently, we conclude that the gneissic granite was formed at 2191–2138 Ma, with a few zircon records of later magmatic events. The porphyritic granite was formed at 1887–1852 Ma and preserved inherited zircons with ages of ~2175 Ma and ~2625 Ma (Figure 7a,b).

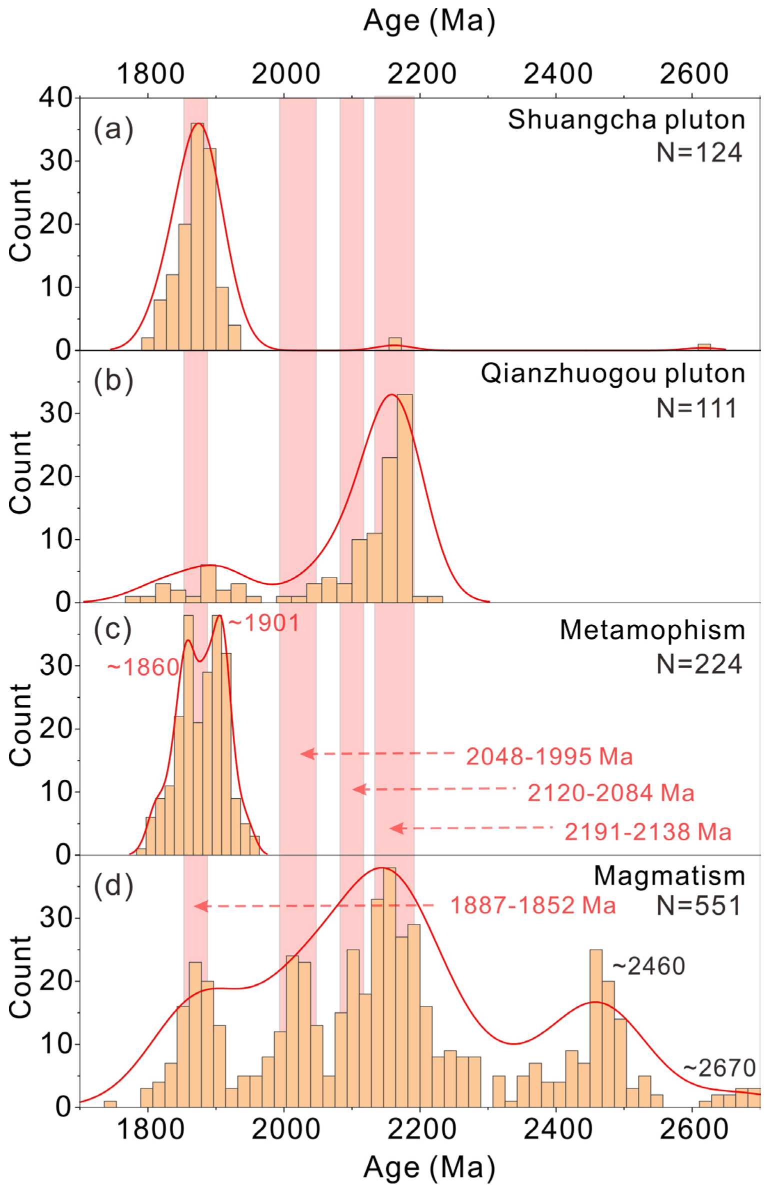

Figure 7. Age spectra (Ma) for zircons from the Ji'an Group and related granites. (**a**) Magmatic zircons of the porphyritic granite (Shuangcha pluton); (**b**) magmatic zircons of the gneissic granite (Qianzhuogou pluton); (**c**) metamorphic zircons of the Ji'an Group; (**d**) detrital zircons of the Ji'an Group. Data from [9,34,35,38,43,48] (Supplementary File).

In this study, the maximum peak age of metamorphic zircons in the metasedimentary rocks was used to represent the minimum depositional age (>1901 Ma). Combined with the minimum peak ages of detrital zircons, the deposition ages for the Mayihe, Huangchagou and Dadongcha formations can be constrained to be 2141–1946, 2117–1917 and 2017–1917 Ma, respectively (Figure 8). These ages are similar to the depositional ages suggested by other authors [33–35].

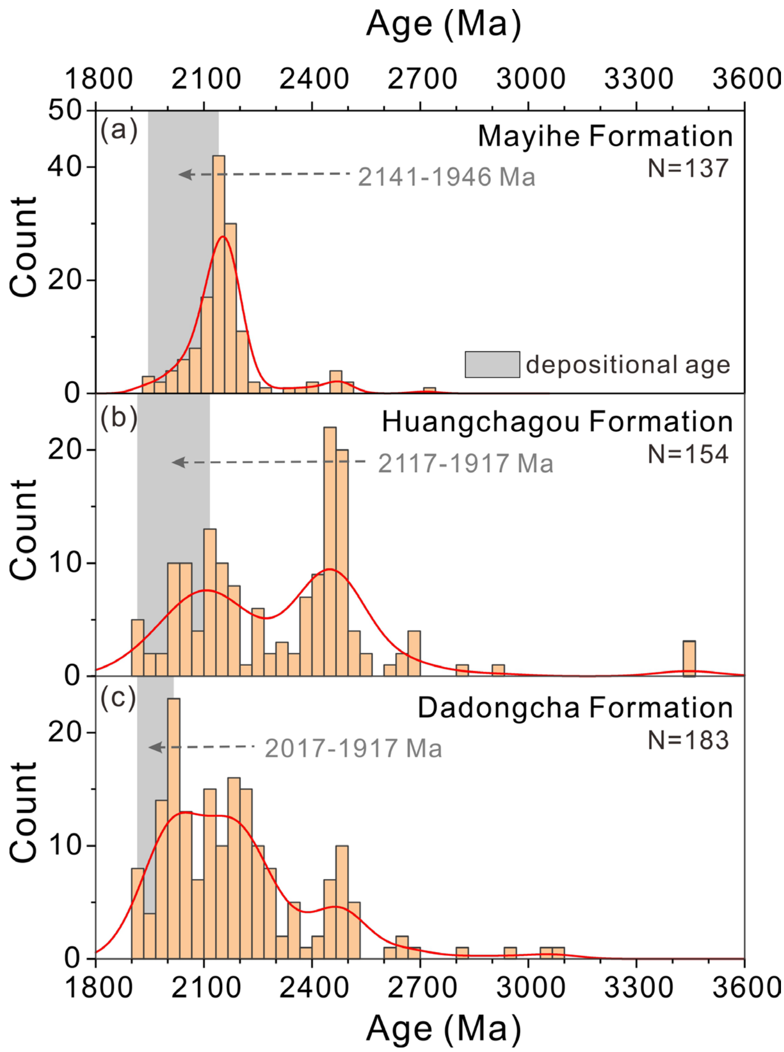

Figure 8. Relative probability diagrams for detrital zircon age data obtained from the (**a**) Mayihe Formation, (**b**) Huangchagou Formation and (**c**) Dadongcha Formation. Data from [9,34,35,38,43,48].

7. Discussion

7.1. Magmatism

The detrital zircons (Th/U > 0.4) in the metasedimentary and meta-igneous rocks, as well as the magmatic zircons in the granites, have preserved consistent ages ranging from 2200 Ma to 1800 Ma, with four periods of magmatism at 2191–2138 Ma, 2120–2084 Ma, 2048–1995 and 1887–1852 Ma. Surprisingly, these magmatic events were also recorded in Paleoproterozoic igneous rocks in the JLJB, as follows: ~2190–2160 Ma: calc-alkaline andesitic–rhyolitic tuffs, A2-type gneissic monzogranite, syenogranite and albite granite [9,38,49]; ~2160–2110 Ma: tholeiitic mafic rocks, metagabbro/diabase and amphibolite [31,32,50]; ~2110–2080 Ma: K-feldspar granite, albite granite and monzogranite [51–54]; ~2000 Ma granites [9]; and ~1870 Ma: granitoids, porphyritic granite and intermediate alkaline rocks [38,51,55]. The composition of these igneous rocks and metavolcanic rocks can be used to assess potential tectonic environments. The calc-alkaline igneous associations (andesitic–rhyolitic tuffs) can be associated with an earlier subduction event [9]. The metavolcanic rocks from the lower part of the Ji'an Group exhibit continuously varying compositions from basalt and andesite to rhyolite, which are typical assemblages of continental volcanic arcs [56]. The gneissic granite (Qianzhuogou pluton) is a highly fractionated, aluminous A2-type granite, which is probably produced in an extensional setting caused by slab rollback during the early stage of subduction. The tholeiitic mafic rocks are related to a back-arc extension [31]. The porphyritic granite (Shuangcha pluton) is an S-type granite formed in a post-collisional extension [9]. To further confirm the tectonic setting of the igneous rocks, the chemical compositions of granites were plotted on the tectonic discrimination diagrams suggested by Pearce et al. [57]. As shown in the Nb–Y tectonic-setting discrimination diagram (Figure 9a), the porphyritic granite (Shuangcha pluton) and gneissic granite (Qianzhuogou pluton) are plotted in the volcanic arc and within plate granite fields. In the Th/Yb–Ta/Yb diagram, metavolcanic rocks fall mainly in the active continental margin and within-plate volcanic zones (Figure 9b). It is speculated that the regional igneous rocks are productions of magmatism under a subduction–back-arc extension–collision system that occurred between 2200 and 1800 Ma.

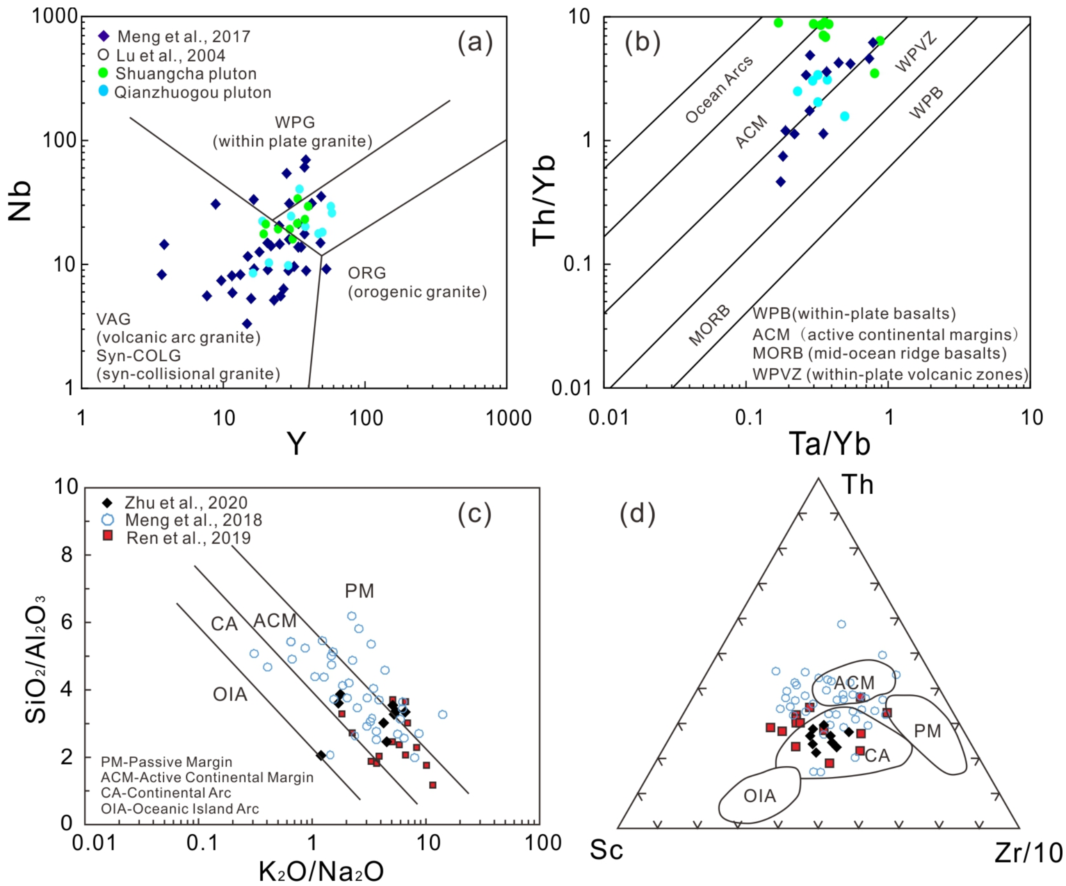

Figure 9. Discrimination diagrams of the metamorphic rocks and granites in the Qinghe area, Tonghua. (**a**) Y versus Nb diagram for the granites in the study area [57]. ORG: Orogenic granite; syn-COLG: syn-collisional granite; VAG: volcanic arc granite; WPG: within-plate granite; (**b**) Th/Yb versus Ta/Yb variation diagrams for the metavolcanic rocks; (**c**) SiO_2/Al_2O_3-K_2O/Na_2O; (**d**) Th-Sc-Zr/10 [47]. PM—Passive margin; ACM—active continental margin; CA—continental arc; OIA—oceanic island arc. Data sources: [33,35,38,43,46].

7.2. Sedimentation

The Ji'an Group consists of thick metasedimentary and meta-igneous successions. Special immobile major and trace elements can be used to discuss protolith composition, provenance and tectonic settings [47]. In the SiO_2/Al_2O_3–K_2O/Na_2O diagram, most samples are plotted in an active continental margin (ACM), and a small number are plotted in the passive margin (PM) and the evolved island arc (A2) area (Figure 9a [47]). In the Th–Sc–Zr/10 discrimination diagrams [47], the samples are mainly plotted in the continental arc (CA) and ACM areas (Figure 9b). The protoliths of the metasedimentary rocks are sets of shale, wacke, arkose, quartz sandstone and carbonate (Figure 6d). The terrigenous sediments may have formed along a passive margin. Moreover, the La/Th-Hf source rock discrimination diagram suggests that the materials were mainly from an arc source with the addition of ancient sediments (Figure 10; [58]). Combined with information from the tectonic setting diagrams, the sediments in the JLJB may have undergone a transformation of the tectonic environment from the passive margin to an active continental margin.

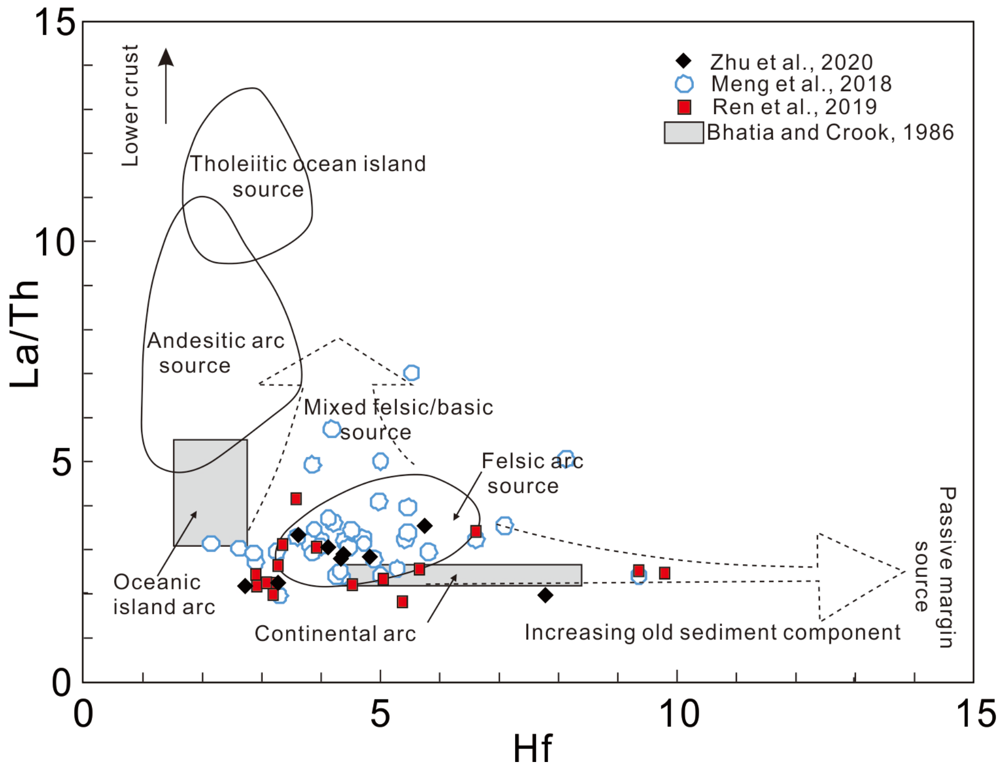

Figure 10. La/Th-Hf source rock discrimination diagram for the metasedimentary rocks in the Qinghe, Tonghua area (after [58]). Data sources: [33,35,46].

The U–Pb ages of detrital zircons are potential indicators of sedimentary provenance and crustal evolution [59]. The detrital zircons in the metasedimentary rocks sampled in the JLJB yield ages of 2191–1995 Ma (Figure 7d). Considering that there are 2.2–2.06 Ga A-type granites and high-K calc-alkaline granites in the Ji'an Group [10], we speculate that the Paleoproterozoic granites were the main material source. According to records of the Neo-Archean metamorphic basement in the Longgang block [11], a few ages of 2.5 Ga, 2.7 Ga, 3.1 Ga and 3.5 Ga may indicate the contribution of fragments of the Neo-Archean metamorphic granitic gneiss to the Ji'an Group. These ages could also result from sediment recycling. The recycling of detrital zircons does not alter the U–Pb age spectra of detrital zircon populations [60]. However, the relative probability diagrams for detrital zircon age data obtained from the Ji'an Group and sedimentary rocks in the JLJB [9] display distinct age spectra.

In addition, zircon Hf isotopes can effectively reflect the source properties (juvenile crust, ancient crust or depleted mantle; [61]). This paper summarizes the zircon Hf isotopes of miscellaneous metamorphic rocks and granites in the Ji'an Group. According to the εHf (t)-T diagram, the metasedimentary rocks of the Ji'an Group have εHf values between −10 and 5, which mainly originate from the recycling of an ancient crust, including Paleoproterozoic granites, coeval differentiated volcanic rocks and small amounts of Archean granites. The metavolcanic rocks of the Ji'an Group have positive εHf values of 2–7 and show low SiO_2 and high contents of FeO^T, MgO, CaO, Cr, Co and Ni, which were predominantly derived from the depleted mantle [33,42,43]. The gneissic granites (Qianzhuogou pluton) have εHf values of between −3 and 3, similarly to some of the metamorphic rocks. We infer that the gneissic granites are derived from both Archean TTG gneisses and the metamorphic basement of the ancient upper crust. The porphyritic granites show similar εHf values to metasedimentary rocks and are more likely to be derived from productions of the partial melting of metapelites (Figure 11). The resulting partial melting of the mantle and crust may reflect a convergent setting.

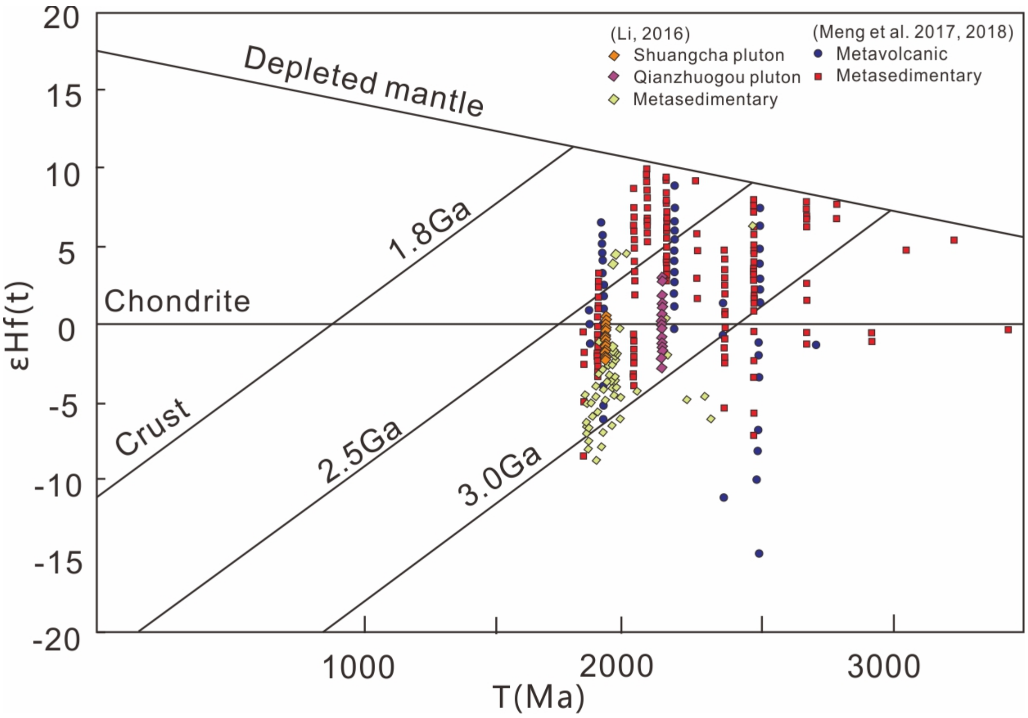

Figure 11. Zircon Hf isotope characteristics of metamorphic rocks of the Ji'an Group and Paleoproterozoic granites. Data sources: [33,42,43].

The convergent settings have a high proportion of detrital zircons (statistically generally greater than 50%) with ages close to the age of the sediment. Combined with stratigraphy, tectonics and geochemistry, high-quality detrital zircon spectra can reflect the tectonic setting [62]. Stratigraphically, the Ji'an Group can be associated with the Laoling Group. The Ji'an Group is located in the south of the Tonghua area and is mainly composed of aluminous schist, pelitic gneiss, felsic gneiss, granulite and interlayered marble and quartzite. The Laoling Group is mainly located in the north of the Tonghua area. The rock types of the Dataishan and Zhenzhumen formations in the Laoling group mainly include quartzite, felsic granulite and marble. We have compiled detrital zircon data from the metasedimentary rocks in the Ji'an Group and plotted them with depositional ages of 2140, 2120 and 2020 Ma from the Mayihe, Huangchagou and Dadongcha formations [33–35]. The dataset suggests that the Ji'an Group was formed in a convergent setting (CA − DA < 100 Ma at 30% of the zircon population). Furthermore, detrital zircon ages closely resemble the Mt Isa basin (Figure 12), which is a typical back-arc basin setting [63]. Detrital zircon data from the Dataishan and Zhenzhumen formations reflect an extensional setting (CA − DA > 150 Ma at 5% of the zircon population), such as a passive margin (Figure 12). Combined with the stratigraphic rock assemblage and detrital zircon, the Ji'an and Laoling Groups were deposited at the same time in different areas during the early stage and later switched to deposit in layers with each other. During the early stage, the Ji'an Group was deposited on the continental arc side, and the Laoling Group was deposited on the passive margin side. During the late stage, both groups were deposited in a back-arc basin setting [20].

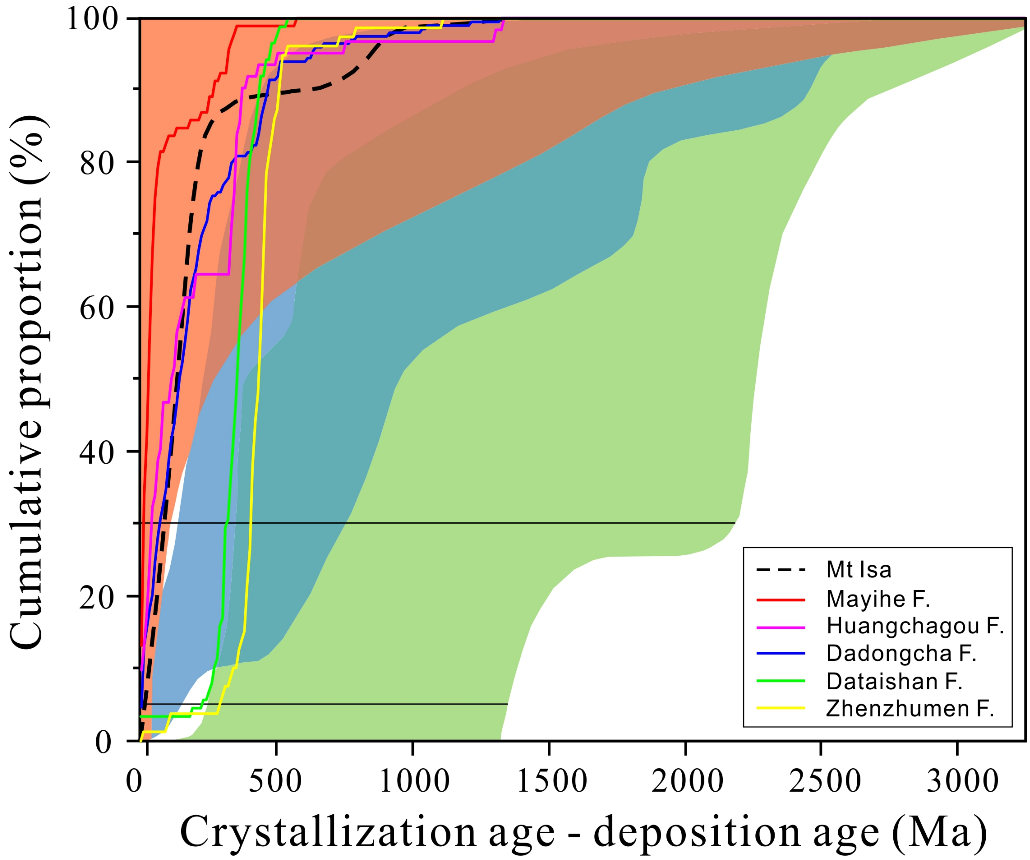

Figure 12. Cumulative proportion diagrams of samples from the Ji'an Group and Laoling Group to constrain their depositional settings (convergent: red field; collisional: blue field; extensional basins: green field [62]). Data sources: [33–35,38,42,48].

7.3. Metamorphism and Anatexis

Some studies on the metamorphic evolution of the Ji'an and South Liaohe Groups obtained low-pressure near-isobaric cooling (IBC) anticlockwise P–T paths, which were previously attributed to a post-orogenic thermal event related to the underplating of mantle magmas [24], whereas recent studies on the Al-rich gneisses showed that they experienced granulite-facies metamorphism and display a near-isothermal decompression (ITD) clockwise P–T path, which is better explained by a subduction/collision model rather than a single rift model [37,64,65]. Whether the metamorphic evolution of the JLJB is a clockwise or an anticlockwise P–T path (an isobaric cooling or an isothermal decompression) remains controversial.

As the metamorphic zircons in the Ji'an Group show (Figure 7c), there may have been two periods of metamorphic events during the formation of the JLJB. Four periods of magmatism and the 1.90–1.80 Ga syn-collisional granites also indicate the possibility of more than one metamorphic event. In addition, the garnet on the prograde clockwise path and cordierite-bearing assemblages on the post-exhumation cooling anticlockwise path fit better with the petrography and growth of cordierite after garnet. These results suggest the existence of superposed clockwise and anticlockwise P–T paths in the JLJB due to the temporal and spatial disparities in an orogenic system [66]. During 1.95–1.90 Ga, the collisional assembly of the Longgang and Nangrim blocks within the NCC was associated with an HP granulite-facies metamorphism. The subsequent exhumation of the orogenic root and regional extension resulted in decompression melting during 1.90–1.86 Ga [67], producing metamorphism with an isothermal decompression clockwise P–T path. Meanwhile, the ascent of the orogenic root was compensated by the contemporaneous descent of part of the upper–middle crustal materials [66]. These downward-moving materials were heated by synchronous extensive anatexis, hot orogenic root and shear heating, triggering the significant heating with a pressure increase and producing metamorphism with an isobaric cooling anticlockwise P–T path at 1.86–1.80 Ga.

Anatexis is a common consequence of high-grade metamorphism. With the discovery of 1.90–1.86 Ga granulite-facies metamorphism in the Ji'an Group, regional anatexis is also found throughout the Ji'an Group [11]. The ages of the anatectic zircons in the Ji'an Group and Jiaobei area suggest that anatectic melt crystallization (cooling stage) occurred at 1.86–1.84 Ga [11,35]. In addition, the U–Pb dating of monazites yielded a peak age of 1.85 Ga [36], which is also interpreted as the timing of melt crystallization during isobaric cooling. All of these findings suggest that the metamorphic history can be reduced to a granulite-facies peak metamorphism, followed by a near-isothermal decompression, and finally a post-exhumation isobaric cooling to amphibolite-facies retrograde metamorphism.

7.4. Evolution of the JLJB

The JLJB has experienced multiple stages of metamorphic–deformational and magmatic–tectonic events [9,14–17,19,20,34,36,37,49,54]. These events have made reconstructing the tectonic evolution of the JLJB extremely challenging. However, recent intensive studies have allowed for the creation of a broad summary of the tectonic evolution model of the JLJB, consisting of the following four main models: (1) the intracontinental rift opening and closing model based on the occurrence of A-type granites, bimodal volcanics, basic intrusions and metamorphism with anticlockwise P–T paths [25,26,39,49,52–54,68–71]; (2) the continent–arc–continent collision model supported by high-pressure granulite, volcanic arc rocks, basic dikes and clockwise P–T paths [27,28,31,52,71,72]; (3) the rift–subduction–collision cycle model based on the HP pelitic granulites, clockwise P–T paths and a basin-controlling boundary fault [10,12,29,73–75]; (4) the back-arc basin opening and closing model supported by the geochemical studies of ca. 2.2–2.1 Ga mafic–granitic intrusions and detrital zircons of sedimentary rocks within the JLJB [31,32,50,55,76,77].

To resolve the controversy, we discuss these proposed constraints by contrasting them with those possibilities based on the geochronology and tectonic setting of the sedimentation, metamorphism and magmatism in the JLJB. The ~2190 Ma calc-alkaline basalt–andesite–rhyolites (protoliths of the meta-igneous rocks) formed a continuous magmatic sequence rather than bimodal volcanic rocks formed in an intracontinental rift. The ~2160 Ma gneissic granites were A2-type granites formed in a back-arc extensional environment rather than A1-type granites formed in a rift environment. The ~2140–1950 Ma sedimentary rocks were deposited in a passive margin-back-arc basin setting rather than in a rift. The ~1900–1800 Ma metamorphic events show granulite-facies metamorphism with a clockwise isothermal decompression P–T path, followed by amphibolite-facies metamorphism with an anticlockwise isobaric cooling P–T path, implying that the JLJB underwent a subduction–collision–extension rather than a single rift model.

Combining these observations with the sedimentation, metamorphism and magmatism identified in the JLJB, we suggest a subduction–back-arc basin extension–collision–exhumation model for the evolution of the JLJB. The gneissic granite (Qianzhuogou pluton) and protoliths of the meta-igneous rocks (e.g., calc-alkaline basalt, andesite, dacite and rhyolite) in the Ji'an Group were formed in a subduction–back-arc basin extensional environment at ~2.2–2.16 Ga. Following this, a sequence of shales, wakes and arkoses were deposited in a continental back-arc basin at ~2.14 Ga, related to the protoliths of the metasedimentary rocks of the Ji'an Group. Later, these sediments were involved in the continent–arc–continent collision between the Longgang and Nangrim blocks at ~1.95 Ga, at which point the peak metamorphism occurred at 1.90 Ga, and isothermal decompression melting occurred during the post-collisional extension at 1.86 Ga. Meanwhile, the porphyritic granite (Shuangcha pluton) was formed in the resulting extensional environment. Finally, the post-exhumation isobaric cooling stage occurred at 1.86–1.80 Ga (Figure 13).

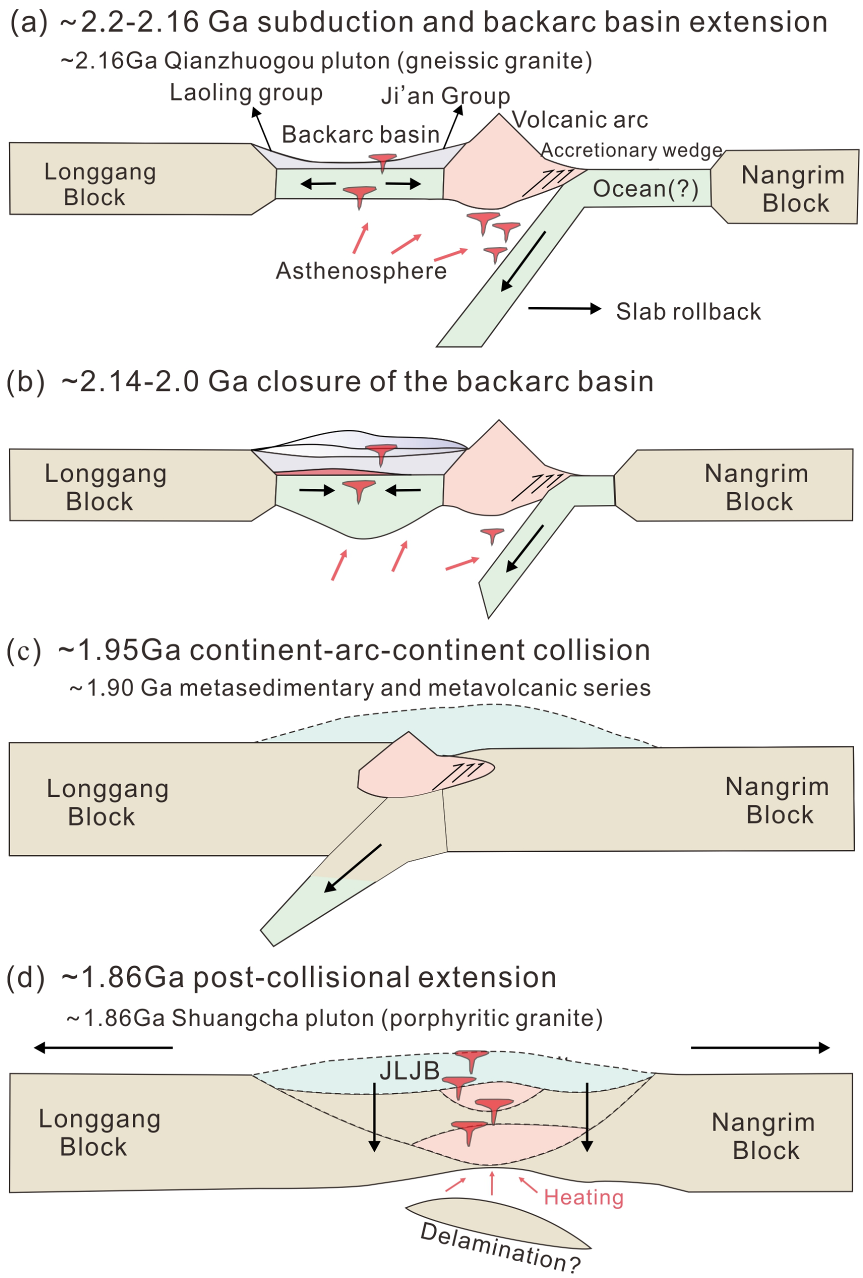

Figure 13. Tectonic evolution model of the JLJB.

8. Conclusions

Based on a systematic investigation of the previous sources, this paper presents an overview of the formation and evolution of the Ji'an Group and the JLJB. The protoliths of the metasedimentary rocks of the Ji'an Group consist of shale, wacke, arkose, quartzite and carbonate, while the meta-igneous rocks consist of continuous calc-alkaline basalt–andesite–dacite–rhyolite. These sediments were formed in an active continental margin and back-arc environment at 2.2–2.0 Ga and were involved in a continent–arc–continent collision between the Longgang and Nangrim blocks in the NCC at ~1.95 Ga. The collision coincidentally led to the closure of the back-arc basin and resulted in regional HP metamorphism at ~1.90 Ga, followed by isothermal decompression melting. The crustal anatexis triggered the 1.86 Ga MP metamorphism and subsequent post-exhumation isobaric cooling at 1.86–1.80 Ga.

Supplementary Materials: The following supporting information can be downloaded at https://www.mdpi.com/article/10.3390/min13070835/s1. Table S1: Age summary of the Ji'an Group and related granites.

Author Contributions: E.Z. conceptualization, methodology, data curation, investigation and writing—original draft preparation; C.L. supervision, funding acquisition, investigation and writing—review and editing; C.Z., X.X. and Y.Y. writing—review and editing. All authors have read and agreed to the published version of the manuscript.

Funding: This study was financially supported by the National Natural Science Foundation of China (No. 41972215, 42172213 and 41872192).

Data Availability Statement: All data used in this study are available in the main text and in the Supplementary Materials.

Acknowledgments: We are grateful to Xiaolei Sun, Dongxue Li, Shiju Jia, Zhiwei Song and Shuyue Qu of the College of Earth Sciences, Jilin University, for their advice and assistance that helped to improve the manuscript. We thank Qi Zheng from the School of Foreign Language Education, Jilin University, for the linguistic review, which significantly improved the manuscript.

Conflicts of Interest: We declare that we do not have any commercial or associative interest that represents conflict of interest in connection with the manuscript submitted.

Appendix A

Table A1. Sample summary of the Ji'an Group.

Sample	Description	Note	Method	References
TH1101-9	graphitic felsic gneiss	Dadongcha Formation	major element	[42]
TH1102-1	felsic gneiss	Dadongcha Formation	major element	[42]
TH1126-1	graphitic felsic gneiss	Huangchagou Formation	major element	[42]
TH1101-1	mica-schist	Dadongcha Formation	major element	[42]
TH1108-1	mica-schist	Dadongcha Formation	major element	[42]
TH1109-1	andalusite mica schist	Huangchagou Formation	major element	[42]
TH1119-1	garnet-sillimanite-cordierite gneiss	Dadongcha Formation	major element	[42]
TH1119-2	garnet-sillimanite-cordierite gneiss	Dadongcha Formation	major element U–Pb Age	[42]
TH1130-1	garnet-sillimanite gneiss	Dadongcha Formation	major element	[42]
TH1130-2	garnet-sillimanite gneiss	Dadongcha Formation	Lu–Hf isotopic data	[42]
TH1135-1	garnet-sillimanite gneiss	Dadongcha Formation	major element	[42]
TH1138-2	garnet-biotite gneiss	Dadongcha Formation	major element	[42]
TH1105-4	hypersthene-amphibole granulite	Huangchagou Formation	major element U–Pb Age	[42]
TH1107-2	amphibole plagioclase gneiss	Huangchagou Formation	major element	[42]
TH1129-6	amphibole plagioclase gneiss	Mayihe Formation	major element	[42]
TH1123-1	diopside marble	Huangchagou Formation	major element Lu–Hf isotopic data U–Pb Age	[42]
TH1104-1	biotite monzonitic granite	Qianzhuogou pluton	major element	[42]
TH1106-1	monzonitic granite	Qianzhuogou pluton	major element Lu–Hf isotopic data U–Pb Age	[42]
TH1121-1	monzonitic granite	Qianzhuogou pluton	major element	[42]
TH1125-1	porphyritic garnet granite	Qianzhuogou pluton	major element	[42]
TH1118-1	porphyritic garnet granite	Shuangcha pluton	major element Lu–Hf isotopic data U–Pb Age	[42]
TH1120-1	porphyritic garnet granite	Shuangcha pluton	major element	[42]
TH1122-1	porphyritic garnet granite	Shuangcha pluton	major element Lu–Hf isotopic data U–Pb Age	[42]
S6-3	garnet-bearing biotite-plagioclase gneiss	Dadongcha Formation	major and trace element U–Pb Age	[35]
S10-2	garnet-biotite schist	Dadongcha Formation	major and trace element	[35]
S57-2	hypersthene-spinel-cordierite-biotite gneiss	Dadongcha Formation	major and trace element	[35]

Table A1. *Cont.*

Sample	Description	Note	Method	References
S24-1	garnet-sillimanite-cordierite-biotite gneiss	Dadongcha Formation	major and trace element U–Pb Age	[35]
ddc-1	garnet-sillimanite-cordierite-biotite gneiss	Dadongcha Formation	major and trace element U–Pb Age	[35]
ddc-2	garnet-sillimanite-cordierite-biotite gneiss	Dadongcha Formation	major and trace element U–Pb Age	[35]
S30-3	garnet-sillimanite-cordierite-biotite gneiss	Dadongcha Formation	major and trace element U–Pb Age	[35]
J1076-1	garnet-sillimanite-cordierite-biotite gneiss	Dadongcha Formation	major and trace element U–Pb Age	[35]
J1082-3	garnet-sillimanite-cordierite-biotite gneiss	Dadongcha Formation	major and trace element U–Pb Age	[35]
09LJ22-1	garnet-sillimanite-biotite gneiss	Ji'an Group	major and trace element	[46]
09LJ22-2	garnet-sillimanite-biotite gneiss	Ji'an Group	major and trace element	[46]
09LJ22-3	garnet-sillimanite-biotite gneiss	Ji'an Group	major and trace element	[46]
09LJ23	garnet-sillimanite-biotite gneiss	Ji'an Group	major and trace element	[46]
12LJ21	garnet-sillimanite-biotite gneiss	Ji'an Group	major and trace element	[46]
09LJ25-1	garnet-sillimanite-biotite gneiss	Ji'an Group	major and trace element	[46]
09LJ25-3	garnet-sillimanite-biotite gneiss	Ji'an Group	major and trace element	[46]
13LJ22-2	garnet-sillimanite-biotite gneiss	Ji'an Group	major and trace element	[46]
09LJ14	mica-schist	Ji'an Group	major and trace element	[46]
09LJ14-2	mica-schist	Ji'an Group	major and trace element	[46]
09LJ14-3	mica-schist	Ji'an Group	major and trace element	[46]
09LJ14-4	mica-schist	Ji'an Group	major and trace element	[46]
11LJ16-1	mica-schist	Ji'an Group	major and trace element	[46]
12LJ29	sericite phyllite	Ji'an Group	major and trace element	[46]
JA10-2	metavolcanic rocks	Ji'an Group	major and trace element	[33]
JA11-1	metavolcanic rocks	Ji'an Group	major and trace element	[33]
JA11-2	metavolcanic rocks	Ji'an Group	major and trace element	[33]
JA06-1	metavolcanic rocks	Ji'an Group	major and trace element	[33]
JA07-2	metavolcanic rocks	Ji'an Group	major and trace element	[33]
TH26-1	amphibole-bearing biotite–plagioclase gneiss	Ji'an Group	major and trace element Lu–Hf isotopic data U–Pb Age	[33]
TH28-1	metavolcanic rocks	Ji'an Group	major and trace element	[33]
TH31-1	metavolcanic rocks	Ji'an Group	major and trace element	[33]
TH31-2	metavolcanic rocks	Ji'an Group	major and trace element	[33]
TH32-2	metavolcanic rocks	Ji'an Group	major and trace element	[33]
TH36-1	metavolcanic rocks	Ji'an Group	major and trace element	[33]
TH36-2	metavolcanic rocks	Ji'an Group	major and trace element	[33]
TH36-3	metavolcanic rocks	Ji'an Group	major and trace element	[33]
TH38-1	metavolcanic rocks	Ji'an Group	major and trace element	[33]
TH38-2	metavolcanic rocks	Ji'an Group	major and trace element	[33]
TH38-3	metavolcanic rocks	Ji'an Group	major and trace element	[33]
TH38-4	metavolcanic rocks	Ji'an Group	major and trace element	[33]
TH41-1	metavolcanic rocks	Ji'an Group	major and trace element	[33]
TH41-2	metavolcanic rocks	Ji'an Group	major and trace element	[33]
TH41-3	metavolcanic rocks	Ji'an Group	major and trace element	[33]
TH42-1	metavolcanic rocks	Ji'an Group	major and trace element	[33]
TH42-3	metavolcanic rocks	Ji'an Group	major and trace element	[33]
TH46-2	metavolcanic rocks	Ji'an Group	major and trace element	[33]
TH47-1	metavolcanic rocks	Ji'an Group	major and trace element	[33]
TH47-2	metavolcanic rocks	Ji'an Group	major and trace element	[33]
TH48-2	felsic gneiss	Ji'an Group	major and trace element Lu–Hf isotopic data U–Pb Age	[33]
TH48-1	amphibolite	Ji'an Group	major and trace element U–Pb Age	[33]
TH50-2	metavolcanic rocks	Ji'an Group	major and trace element	[33]
TH52-2	metavolcanic rocks	Ji'an Group	major and trace element	[33]
TH53-3	metavolcanic rocks	Ji'an Group	major and trace element Lu–Hf isotopic data U–Pb Age	[33]
TH53-4	metavolcanic rocks	Ji'an Group	major and trace element	[33]
TH55-2	metavolcanic rocks	Ji'an Group	major and trace element	[33]
TH55-3	biotite–plagioclase gneiss	Ji'an Group	major and trace element U–Pb Age	[33]

Table A1. *Cont.*

Sample	Description	Note	Method	References
TH56-1	metavolcanic rocks	Ji'an Group	major and trace element	[33]
TH58-2	metavolcanic rocks	Ji'an Group	major and trace element	[33]
TH58-3	metavolcanic rocks	Ji'an Group	major and trace element	[33]
TH59-1	metavolcanic rocks	Ji'an Group	major and trace element Lu–Hf isotopic data	[33]
TH60-2	metavolcanic rocks	Ji'an Group	major and trace element	[33]
TH60-3	metavolcanic rocks	Ji'an Group	major and trace element	[33]
TH63-1	metavolcanic rocks	Ji'an Group	major and trace element	[33]
TH63-2	metavolcanic rocks	Ji'an Group	major and trace element	[33]
TH27-2	metasedimentary rocks	Ji'an Group	major and trace element	[42]
TH30-1.1	metasedimentary rocks	Ji'an Group	major and trace element	[42]
TH30-1.2	metasedimentary rocks	Ji'an Group	major and trace element	[42]
TH30-2	garnet-bearing biotite felsic gneiss	Huangchagou Formation	major and trace element Lu–Hf isotopic data U–Pb Age	[42]
TH30-5	metasedimentary rocks	Ji'an Group	major and trace element	[42]
TH30-10	metasedimentary rocks	Ji'an Group	major and trace element	[42]
TH30-12	metasedimentary rocks	Ji'an Group	major and trace element	[42]
TH33-1	metasedimentary rocks	Ji'an Group	major and trace element	[42]
TH33-4	metasedimentary rocks	Ji'an Group	major and trace element	[42]
TH35-5	metasedimentary rocks	Ji'an Group	major and trace element	[42]
TH35-6	metasedimentary rocks	Ji'an Group	major and trace element	[42]
TH42-3	amphibole-bearing biotite–plagioclase gneiss	Huangchagou Formation	Lu–Hf isotopic data U–Pb Age	[42]
TH39-1	metasedimentary rocks	Ji'an Group	major and trace element	[42]
TH43-1.1	metasedimentary rocks	Ji'an Group	major and trace element	[42]
TH43-1.2	metasedimentary rocks	Ji'an Group	major and trace element	[42]
TH49-1	biotite–plagioclase gneiss	Dadongcha Formation	major and trace element Lu–Hf isotopic data U–Pb Age	[42]
TH49-5	quartz-bearing mica schist	Dadongcha Formation	Lu–Hf isotopic data U–Pb Age	[42]
TH49-6	metasedimentary rocks	Ji'an Group	major and trace element	[42]
TH51-1	metasedimentary rocks	Ji'an Group	major and trace element	[42]
TH51-2	metasedimentary rocks	Ji'an Group	major and trace element	[42]
TH57-1	metasedimentary rocks	Ji'an Group	major and trace element	[42]
TH57-2	metasedimentary rocks	Ji'an Group	major and trace element	[42]
TH61-1	metasedimentary rocks	Ji'an Group	major and trace element	[42]
TH61-2	metasedimentary rocks	Ji'an Group	major and trace element	[42]
TH61-3	metasedimentary rocks	Ji'an Group	major and trace element	[42]
TH52-1	metasedimentary rocks	Ji'an Group	major and trace element	[42]
TH52-3	metasedimentary rocks	Ji'an Group	major and trace element	[42]
TH52-5	metasedimentary rocks	Ji'an Group	major and trace element	[42]
TH52-6	metasedimentary rocks	Ji'an Group	major and trace element	[42]
TH52-7	metasedimentary rocks	Ji'an Group	major and trace element	[42]
TH52-8	metasedimentary rocks	Ji'an Group	major and trace element	[42]
TH53-1	metasedimentary rocks	Ji'an Group	major and trace element	[42]
TH54-1	metasedimentary rocks	Ji'an Group	major and trace element	[42]
TH54-2	metasedimentary rocks	Ji'an Group	major and trace element	[42]
TH55-1	metasedimentary rocks	Ji'an Group	major and trace element	[42]
JA10-1	metasedimentary rocks	Ji'an Group	major and trace element	[42]
JA06-2	metasedimentary rocks	Ji'an Group	major and trace element	[42]
JA07-1	metasedimentary rocks	Ji'an Group	major and trace element	[42]
JA07-3	metasedimentary rocks	Ji'an Group	major and trace element	[42]
JA07-4	metasedimentary rocks	Ji'an Group	major and trace element	[42]
JA07-5	metasedimentary rocks	Ji'an Group	major and trace element	[42]
Y009	felsic gneiss	Dadongcha Formation	U–Pb Age	[38]
Y016	amphibolite	Huangchagou Formation	U–Pb Age	[38]
Y015	graphitic biotite felsic gneiss	Huangchagou Formation	U–Pb Age	[38]
Y006-1	diopside felsic gneiss	Mayihe Formation	U–Pb Age	[38]
1065	syenogranite	Qianzhuogou pluton	major and trace element U–Pb Age (SHRIMP)	[38]
1057-2	syenogranite	Qianzhuogou pluton	major and trace element	[38]
Lu011	syenogranite	Qianzhuogou pluton	major and trace element	[38]
Lu012	syenogranite	Qianzhuogou pluton	major and trace element U–Pb Age (SHRIMP)	[38]
Lu014	syenogranite	Qianzhuogou pluton	major and trace element	[38]
0007	syenogranite	Qianzhuogou pluton	major and trace element U–Pb Age (SHRIMP)	[38]

Table A1. *Cont.*

Sample	Description	Note	Method	References
0014	syenogranite	Qianzhuogou pluton	major and trace element	[38]
12078	syenogranite	Qianzhuogou pluton	major and trace element	[38]
12084	syenogranite	Qianzhuogou pluton	major and trace element	[38]
42037-2	amphibolite	Qianzhuogou pluton	major and trace element	[38]
0007-1	amphibolite	Qianzhuogou pluton	major and trace element	[38]
Y007-1	amphibolite	Qianzhuogou pluton	major and trace element	[38]
92015	giant porphyritic granite	Shuangcha pluton	U–Pb Age (SHRIMP)	[38]
12082	giant porphyritic granite	Shuangcha pluton	U–Pb Age (SHRIMP)	[38]
Lu010-1	giant porphyritic granite	Shuangcha pluton	U–Pb Age (SHRIMP)	[38]
Lu010-1	giant porphyritic granite	Shuangcha pluton	major and trace element	[38]
Lu010-2	giant porphyritic granite	Shuangcha pluton	major and trace element	[38]
Lu010-3	giant porphyritic granite	Shuangcha pluton	major and trace element	[38]
42040-1	giant porphyritic granite	Shuangcha pluton	major and trace element	[38]
92014	giant porphyritic granite	Shuangcha pluton	major and trace element	[38]
92015	giant porphyritic granite	Shuangcha pluton	major and trace element	[38]
92016	giant porphyritic granite	Shuangcha pluton	major and trace element	[38]
12082	giant porphyritic granite	Shuangcha pluton	major and trace element	[38]
Lu013	giant porphyritic granite	Shuangcha pluton	major and trace element	[38]
NMY01	amphibolite	Mayihe Formation	U–Pb Age	[48]
NMY02	amphibole-plagioclase gneiss	Mayihe Formation	U–Pb Age	[48]
NH01	amphibolite	Huangchagou Formation	U–Pb Age	[48]
ND02	biotite felsic gneiss	Dadongcha Formation	U–Pb Age	[48]
NMY03	gneissic adamellite	Qianzhuogou pluton	U–Pb Age	[48]
NQZ01	gneissic adamellite	Qianzhuogou pluton	U–Pb Age	[48]
NSC01	adamellite	Shuangcha pluton	U–Pb Age	[48]
14TH-42-02	biotite felsic gneiss	Mayihe Formation	major and trace element U–Pb Age	[34]
17TH44-01	garnet bearing biotite plagioclase paragneiss	Mayihe Formation	major and trace element U–Pb Age	[34]
17TH-48-01	amphibole-bearing plagioclase paragneiss	Huangchagou Formation	major and trace element U–Pb Age	[34]
17TH-34-01	biotite K-feldspar plagioclase paragneiss	Dadongcha Formation	major and trace element U–Pb Age	[34]
17TH-35-01	garnet-sillimanite plagioclase paragneiss	Dadongcha Formation	major and trace element U–Pb Age	[34]
17TH-45-01	tourmaline-bearing leptynite	Huangchagou Formation	major and trace element U–Pb Age	[34]
17TH-35-03	garnet-bearing mica schist	Dadongcha Formation	major and trace element	[34]

References

1. Hoffman, P.F. United Plates of America, The Birth of a Craton: Early Proterozoic Assembly and Growth of Laurentia. *Annu. Rev. Earth Planet. Sci.* **1988**, *16*, 543–603. [CrossRef]
2. Roberts, N.M.W. The boring billion?—Lid tectonics, continental growth and environmental change associated with the Columbia supercontinent. *Geosci. Front.* **2013**, *4*, 681–691. [CrossRef]
3. Zhao, G.; Cawood, P.A.; Wilde, S.A.; Sun, M. Review of global 2.1–1.8 Ga orogens: Implications for a pre-Rodinia supercontinent. *Earth-Sci. Rev.* **2002**, *59*, 125–162. [CrossRef]
4. Faure, M.; Trap, P.; Lin, W.; Monié, P.; Bruguier, O. The formation of the North China Craton by two Palaeoproterozoic continental collisions in Lüliang-Hengshan-Wutaishan-Fuping massifs. *Episodes* **2007**, *30*, 1–12. [CrossRef]
5. Kusky, T.M.; Li, J. Paleoproterozoic tectonic evolution of the North China Craton. *J. Asian Earth Sci.* **2003**, *22*, 383–397. [CrossRef]
6. Zhao, G.C.; Sun, M.; Wilde, S.A.; Li, S.Z. Late Archean to Paleoproterozoic evolution of the North China Craton: Key issues revisited. *Precambrian Res.* **2005**, *136*, 177–202. [CrossRef]
7. Zhao, G.; Wilde, S.A.; Cawood, P.A.; Lu, L. Thermal Evolution of Archean Basement Rocks from the Eastern Part of the North China Craton and Its Bearing on Tectonic Setting. *Int. Geol. Rev.* **1998**, *40*, 706–721. [CrossRef]
8. Liu, D.Y.; Nutman, A.P.; Compston, W.; Wu, J.S.; Shen, Q.H. Remnants of ≥3800 Ma crust in the Chinese part of the Sino-Korean craton. *Geology* **1992**, *20*, 339–342. [CrossRef]
9. Xu, W.; Liu, F. Geochronological and geochemical insights into the tectonic evolution of the Paleoproterozoic Jiao-Liao-Ji Belt, Sino-Korean Craton. *Earth-Sci. Rev.* **2019**, *193*, 162–198. [CrossRef]
10. Zhao, G.C.; Cawood, P.A.; Li, S.Z.; Wilde, S.A.; Sun, M.; Zhang, J.; He, Y.H.; Yin, C.Q. Amalgamation of the North China Craton: Key issues and discussion. *Precambrian Res.* **2012**, *222–223*, 55–76. [CrossRef]
11. Liu, F.L.; Liu, P.H.; Wang, F.; Liu, C.H.; Cai, J. Progresses and overviews of voluminous meta-sedimentary series within the Paleoproterozoic Jiao–Liao–Ji orogenic/mobile belt, North China Craton. *Acta Petrol. Sin.* **2015**, *31*, 2816–2846, (In Chinese with English Abstract).

12. Zhai, M.-G.; Santosh, M. The early Precambrian odyssey of the North China Craton: A synoptic overview. *Gondwana Res.* **2011**, *20*, 6–25. [CrossRef]
13. Lee, B.C.; Oh, C.W.; Wang, X. Paleoproterozoic (ca. 1.87–1.69 Ga) arc-related tectonothermal events on northcentral Yeongnam Massif, South Korea and its tectonic implications: Insights from metamorphism, geochemistry and geochronology. *Precambrian Res.* **2020**, *338*, 105562. [CrossRef]
14. Li, Z.; Chen, B.; Yan, X. The Liaohe Group: An insight into the Paleoproterozoic tectonic evolution of the Jiao–Liao–Ji Belt, North China Craton. *Precambrian Res.* **2019**, *326*, 174–195. [CrossRef]
15. Liu, J.; Zhang, J.; Liu, Z.; Yin, C.; Xu, Z.; Cheng, C.; Zhao, C.; Wang, X. Late Paleoproterozoic crustal thickening of the Jiao–Liao–Ji belt, North China Craton: Insights from ca. 1.95–1.88 Ga syn-collisional adakitic granites. *Precambrian Res.* **2021**, *355*, 106120. [CrossRef]
16. Liu, J.; Zhang, J.; Yin, C.; Cheng, C.; Liu, X.; Zhao, C.; Chen, Y.; Wang, X. Synchronous A-type and adakitic granitic magmatism at ca. 2.2 Ga in the Jiao–Liao–Ji belt, North China Craton: Implications for rifting triggered by lithospheric delamination. *Precambrian Res.* **2020**, *342*, 105629. [CrossRef]
17. Liu, P.H.; Liu, F.L.; Tian, Z.-H.; Cai, J.; Ji, L.; Wang, F. Petrological and geochronological evidence for Paleoproterozoic granulite-facies metamorphism of the South Liaohe Group in the Jiao-Liao-Ji Belt, North China Craton. *Precambrian Res.* **2019**, *327*, 121–143. [CrossRef]
18. Wang, X.; Oh, C.W.; Lee, B.C.; Liu, F. Paleoproterozoic postcollisional metamorphic and igneous activities in the Jinan area of the Jiao-Liao-Ji Belt in the North China Craton and their tectonic implications. *Precambrian Res.* **2020**, *346*, 105793. [CrossRef]
19. Xu, W.; Liu, F.; Wang, F.; Santosh, M.; Dong, Y.; Li, S. Palaeoproterozoic tectonic evolution of the Jiao–Liao–Ji Belt, North China Craton: Geochemical and isotopic evidence from ca. 2.17 Ga felsic tuff. *Geol. J.* **2020**, *55*, 409–424. [CrossRef]
20. Zhang, W.; Liu, P.; Xu, W.; Tian, Z.; Zhou, W.; Wang, Y.; Zhang, Y.; Wang, W. Petrogenesis and implications of ~2.1 Ga Jingqishan granites in the Jiaobei Terrane, North China Craton. *Precambrian Res.* **2022**, *369*, 106536. [CrossRef]
21. Jahn, B.M.; Liu, D.; Wan, Y.; Song, B.; Wu, J. Archean crustal evolution of the Jiaodong Peninsula, China, as revealed by zircon SHRIMP geochronology, elemental and Nd-isotope geochemistry. *Am. J. Sci.* **2008**, *308*, 232–269. [CrossRef]
22. Lu, X.P.; Wu, F.Y.; Guo, J.H.; Wilde, S.A.; Yang, J.H.; Liu, X.M.; Zhang, X.O. Zircon U–Pb geochronological constraints on the Paleoproterozoic crustal evolution of the Eastern Block in the North China Craton. *Precambrian Res.* **2006**, *146*, 138–164. [CrossRef]
23. Zhou, X.; Zhao, G.; Wei, C.; Geng, Y.; Sun, M. EPMA U-Th-Pb monazite and SHRIMP U-Pb zircon geochronology of high-pressure pelitic granulites in the Jiaobei massif of the North China Craton. *Am. J. Sci.* **2008**, *308*, 328–350. [CrossRef]
24. He, G.P.; Ye, H.W. Two types of Early Proterozoic metamorphism and its tectonic significance in eastern Liaoning and southern Jilin areas. *Acta Petrol. Sin.* **1998**, *14*, 152–162, (In Chinese with English Abstract).
25. Li, S.Z.; Zhao, G.; Sun, M.; Han, Z.; Luo, Y.; Hao, D.; Xia, X. Deformation history of the Paleoproterozoic Liaohe assemblage in the eastern block of the North China Craton. *J. Asian Earth Sci.* **2005**, *24*, 659–674. [CrossRef]
26. Luo, Y.; Sun, M.; Zhao, G.; Li, S.; Xu, P.; Ye, K.; Xia, X. LA-ICP-MS U–Pb zircon ages of the Liaohe Group in the Eastern Block of the North China Craton: Constraints on the evolution of the Jiao-Liao-Ji Belt. *Precambrian Res.* **2004**, *134*, 349–371. [CrossRef]
27. Bai, J. *The Precambrian Geology and Pb–Zn Mineralization in the Northern Margin of North China Platform*; Geological Publishing House: Beijing, China, 1993; (In Chinese with English Abstract).
28. Faure, M.; Lin, W.; Monie, P.; Bruguier, O. Palaeoproterozoic arc magmatism and collision in Liaodong Peninsula (north-east China). *Terra Nova* **2004**, *16*, 75–80. [CrossRef]
29. Zhai, M.; Santosh, M. Metallogeny of the North China Craton: Link with secular changes in the evolving Earth. *Gondwana Res.* **2013**, *24*, 275–297. [CrossRef]
30. Zhao, G.C.; Zhai, M. Lithotectonic elements of Precambrian basement in the North China Craton: Review and tectonic implications. *Gondwana Res.* **2013**, *23*, 1207–1240. [CrossRef]
31. Meng, E.; Liu, F.-L.; Liu, P.-H.; Liu, C.-H.; Yang, H.; Wang, F.; Shi, J.-R.; Cai, J. Petrogenesis and tectonic significance of Paleoproterozoic meta-mafic rocks from central Liaodong Peninsula, northeast China: Evidence from zircon U–Pb dating and in situ Lu–Hf isotopes, and whole-rock geochemistry. *Precambrian Res.* **2014**, *247*, 92–109. [CrossRef]
32. Xu, W.; Liu, F.; Tian, Z.; Liu, L.; Ji, L.; Dong, Y. Source and petrogenesis of Paleoproterozoic meta-mafic rocks intruding into the North Liaohe Group: Implications for back-arc extension prior to the formation of the Jiao-Liao-Ji Belt, North China Craton. *Precambrian Res.* **2018**, *307*, 66–81. [CrossRef]
33. Meng, E.N.; Wang, C.-Y.; Li, Z.; Li, Y.-G.; Yang, H.; Cai, J.I.A.; Ji, L.E.I.; Jin, M.-Q. Palaeoproterozoic metasedimentary rocks of the Ji'an Group and their significance for the tectonic evolution of the northern segment of the Jiao–Liao–Ji Belt, North China Craton. *Geol. Mag.* **2017**, *155*, 149–173. [CrossRef]
34. Zhang, W.; Liu, F.L.; Cai, J.; Liu, C.H.; Liu, J.H.; Liu, P.H.; Liu, L.S.; Wang, F.; Yang, H. Geochemistry, zircon U-Pb dating and tectonic implications of the Palaeoproterozoic Ji'an and Laoling groups, northeastern Jiao-Liao-Ji Belt, North China Craton. *Precambrian Res.* **2018**, *314*, 264–287. [CrossRef]
35. Zhu, E.L.; Liang, C.Y.; Zheng, C.Q.; Yang, Y.; Zhou, X.; Zhang, Q.; Hu, P.Y. Tectonic evolution of the Dadongcha Formation, Ji'an group, Qinghe area, Tonghua, NE China: Implications from geochronological and geochemical evidence of metapelites. *Precambrian Res.* **2020**, *350*, 105917. [CrossRef]
36. Cai, J.; Liu, F.; Liu, P.; Wang, F. Metamorphic P–T evolution and tectonic implications of pelitic granulites in the Ji'an area, northeastern Jiao–Liao–Ji Belt, North China Craton. *J. Asian Earth Sci.* **2020**, *191*, 104197. [CrossRef]

37. Cai, J.; Liu, F.L.; Liu, P.H.; Wang, F.; Meng, E.; Wang, W.; Yang, H.; Ji, L.; Liu, L.S. Discovery of granulite-facies metamorphic rocks in the Ji'an area, northeastern Jiao–Liao–Ji Belt, North China Craton: Metamorphic P–T, evolution and geological implications. *Precambrian Res.* **2017**, *303*, 626–640. [CrossRef]
38. Lu, X.P.; Wu, F.Y.; Lin, J.Q.; Sun, D.Y.; Zhang, Y.B.; Guo, C.L. Geochronological successions of the Early Precambrian granitic magmatism in southern Liaodong Peninsula and its constraints on tectonic evolution of the North China Craton. *Chin. J. Geol.* **2004**, *39*, 123–138, (In Chinese with English Abstract).
39. Li, S.Z.; Zhao, G. SHRIMP U–Pb zircon geochronology of the Liaoji granitoids: Constraints on the evolution of the Paleoproterozoic Jiao-Liao-Ji Belt in the Eastern Block of the North China Craton. *Precambrian Res.* **2007**, *158*, 1–16. [CrossRef]
40. Douce, A.E.; Johnston, A.D. Phase equilibria and melt productivity in the pelitic system: Implications for the origin of peraluminous granitoids and aluminous granulites. *Contrib. Mineral. Petrol.* **1991**, *107*, 202–218. [CrossRef]
41. Vielzeuf, D.; Montel, J.M. Partial melting of metagreywackes. Part I. Fluid-absent experiments and phase relationships. *Contrib. Mineral. Petrol.* **1994**, *117*, 375–393. [CrossRef]
42. Li, X.L. *Metamorphic Evolution and Genesis of the Ji'an Group in the Tonghua Region, Jilin Province*; China University of Geosciences: Beijing, China, 2016; (In Chinese with English Abstract).
43. Meng, E.; Wang, C.Y.; Yang, H.; Cai, J.; Ji, L.; Li, Y.G. Paleoproterozoic metavolcanic rocks in the Ji'an Group and constraints on the formation and evolution of the northern segment of the Jiao-Liao-Ji Belt, China. *Precambrian Res.* **2017**, *294*, 133–150. [CrossRef]
44. Simonen, A. Stratigraphy and sedimentation of the Svecofennidic, Early Archean supracrustal rocks in southwestern Finland. *Bull. Geol. Soc. Finl.* **1953**, *16*, 1–64.
45. Herron, M.M. Geochemical classification of terrigenous sands and shales from core or log data. *J. Sediment. Petrol.* **1988**, *58*, 820–829.
46. Ren, Y.W.; Wang, H.C.; Chu, H. Geochemistry of the metamorphic Al-rich sedimentary series and its constraint on provenance in the Paleoproterozoic Liao-Ji active belt. *Geol. Bull. China* **2019**, *38*, 17.
47. Bhatia, M.R.; Crook, K.A.W. Trace element characteristics of graywackes and tectonic setting discrimination of sedimentary basins. *Contrib. Mineral. Petrol.* **1986**, *92*, 181–193. [CrossRef]
48. Qin, Y.; Chen, D.D.; Liang, Y.H.; Zou, C.M.; Zhang, Q.W.; Bai, L.A. Geochronology of Ji'an group in Tonghua Area, Southern Jilin Province: Earth Science. *J. China Univ. Geosci.* **2014**, *39*, 1587–1599, (In Chinese with English Abstract).
49. Lan, T.-G.; Fan, H.-R.; Yang, K.-F.; Cai, Y.-C.; Wen, B.-J.; Zhang, W. Geochronology, mineralogy and geochemistry of alkali-feldspar granite and albite granite association from the Changyi area of Jiao-Liao-Ji Belt: Implications for Paleoproterozoic rifting of eastern North China Craton. *Precambrian Res.* **2015**, *266*, 86–107. [CrossRef]
50. Xu, W.; Liu, F.; Santosh, M.; Liu, P.; Tian, Z.; Dong, Y. Constraints of mafic rocks on a Paleoproterozoic back-arc in the Jiao-Liao-Ji Belt, North China Craton. *J. Asian Earth Sci.* **2018**, *166*, 195–209. [CrossRef]
51. Liu, J.; Liu, F.; Ding, Z.; Liu, P.; Guo, C.; Wang, F. Geochronology, petrogenesis and tectonic implications of Paleoproterozoic granitoid rocks in the Jiaobei Terrane, North China Craton. *Precambrian Res.* **2014**, *255*, 685–698. [CrossRef]
52. Wang, C.C.; Liu, Y.-C.; Zhang, P.-G.; Zhao, G.-C.; Wang, A.-D.; Song, B. Zircon U–Pb geochronology and geochemistry of two types of Paleoproterozoic granitoids from the southeastern margin of the North China Craton: Constraints on petrogenesis and tectonic significance. *Precambrian Res.* **2017**, *303*, 268–290. [CrossRef]
53. Wang, F.; Liu, F.; Liu, P.; Cai, J.; Schertl, H.-P.; Ji, L.; Liu, L.; Tian, Z. In situ zircon U-Pb dating and whole-rock geochemistry of metasedimentary rocks from South Liaohe Group, Jiao-Liao-Ji orogenic belt: Constraints on the depositional and metamorphic ages, and implications for tectonic setting. *Precambrian Res.* **2017**, *303*, 764–780. [CrossRef]
54. Wang, M.; Liu, S.; Fu, J.; Wang, K.; Guo, R.; Guo, B. Neoarchean DTTG gneisses in southern Liaoning Province and their constraints on crustal growth and the nature of the Liao-Ji Belt in the Eastern Block. *Precambrian Res.* **2017**, *303*, 183–207. [CrossRef]
55. Li, C.; Chen, B.; Li, Z.; Yang, C. Petrologic and geochemical characteristics of Paleoproterozoic monzogranitic gneisses from Xiuyan-Kuandian area in Liaodong Peninsula and their tectonic implications. *Yanshi Xuebao/Acta Petrol. Sin.* **2017**, *33*, 963–977.
56. Gill, J.B. *Orogenic Andesites and Plate Tectonics*; Springer: Berlin/Heidelberg, Germany, 1981; p. xiv+385.
57. Pearce, J.; Harris, N.; Tindle, A. Trace Element Discrimination Diagrams for the Tectonic Interpretation of Granitic Rocks. *J. Petrol.* **1984**, *25*, 956–983. [CrossRef]
58. Floyd, P.A.; Leveridge, B.E. Tectonic environment of the Devonian Gramscatho basin, South Cornwall: Framework mode and geochemical evidence from turbiditic sandstones. *J. Geol. Soc.* **1987**, *144*, 531–542. [CrossRef]
59. Cawood, P.A.; Nemchin, A.A.; Strachan, R.; Prave, T.; Krabbendam, M. Sedimentary basin and detrital zircon record along East Laurentia and Baltica during assembly and breakup of Rodinia. *J. Geol. Soc.* **2007**, *164*, 257–275. [CrossRef]
60. Dickinson, W.R.; Lawton, T.F.; Gehrels, G.E. Recycling detrital zircons: A case study from the Cretaceous Bisbee Group of southern Arizona. *Geology* **2009**, *37*, 503–506. [CrossRef]
61. Wu, F.-Y.; Yang, J.-H.; Wilde, S.A.; Liu, X.-M.; Guo, J.-H.; Zhai, M.-G. Detrital zircon U–Pb and Hf isotopic constraints on the crustal evolution of North Korea. *Precambrian Res.* **2007**, *159*, 155–177. [CrossRef]
62. Cawood, P.A.; Hawkesworth, C.J.; Dhuime, B. Detrital zircon record and tectonic setting. *Geology* **2012**, *40*, 875–878. [CrossRef]
63. Giles, D.; Betts, P.; Lister, G. Far-field continental backarc setting for the 1.80–1.67 Ga basins of northeastern Australia. *Geology* **2002**, *30*, 823–826. [CrossRef]

64. Tam, P.Y.; Zhao, G.C.; Sun, M.; Li, S.Z.; Lizuka, Y.; Ka'iMa, G.S.; Yin, C.Q.; He, Y.H.; Wu, M.L. Metamorphic P–T path and tectonic implications of medium-pressure pelitic granulites from the Jiaobei massif in the Jiao–Liao–Ji Belt, North China Craton. *Precambrian Res.* **2012**, *220–221*, 177–191. [CrossRef]
65. Tam, P.Y.; Zhao, G.C.; Zhou, X.W.; Sun, M.; Guo, J.H.; Li, S.Z.; Yin, C.Q.; Wu, M.L.; He, Y.H. Metamorphic P–T path and implications of high-pressure pelitic granulites from the Jiaobei massif in the Jiao–Liao–Ji Belt, North China Craton. *Gondwana Res.* **2012**, *22*, 104–117. [CrossRef]
66. Zou, Y.; Zhai, M.G.; Santosh, M.; Zhou, L.G.; Zhao, L.; Lu, J.S.; Liu, B.; Shan, H.X. Contrasting P-T-t paths from a Paleoproterozoic metamorphic orogen: Petrology, phase equilibria, zircon and monazite geochronology of metapelites from the Jiao-Liao-Ji Belt, North China Craton. *Precambrian Research* **2018**, *311*, 74–97. [CrossRef]
67. Liu, F.; Liu, L.; Cai, J.; Liu, P.; Wang, F.; Liu, C.; Liu, J. A widespread Paleoproterozoic partial melting event within the Jiao-Liao-Ji Belt, North China Craton: Zircon U-Pb dating of granitic leucosomes within pelitic granulites and its tectonic implications. *Precambrian Res.* **2019**, *326*, 155–173. [CrossRef]
68. Luo, Y.; Sun, M.; Zhao, G.; Li, S.; Ayers, J.C.; Xia, X.; Zhang, J. A comparison of U–Pb and Hf isotopic compositions of detrital zircons from the North and South Liaohe Groups: Constraints on the evolution of the Jiao-Liao-Ji Belt, North China Craton. *Precambrian Res.* **2008**, *163*, 279–306. [CrossRef]
69. Wang, X.; Peng, P.; Wang, C.; Yang, S. Petrogenesis of the 2115Ma Haicheng mafic sills from the Eastern North China Craton: Implications for an intra-continental rifting. *Gondwana Res.* **2016**, *39*, 347–364. [CrossRef]
70. Wang, X.; Peng, P.; Wang, C.; Yang, S.; Söderlund, U.; Su, X. Nature of three episodes of Paleoproterozoic magmatism (2180 Ma, 2115 Ma and 1890 Ma) in the Liaoji belt, North China with implications for tectonic evolution. *Precambrian Res.* **2017**, *298*, 252–267. [CrossRef]
71. Yang, M.; Chen, B.; Yan, C. Paleoproterozoic Gneissic Granites in the Liaoji Mobile Belt, North China Craton: Implications for Tectonic Setting. In *Main Tectonic Events and Metallogeny of the North China Craton*; Zhai, M., Zhao, Y., Zhao, T., Eds.; Springer: Singapore, 2016; pp. 155–180.
72. Yuan, L.; Zhang, X.; Xue, F.; Han, C.; Chen, H.; Zhai, M. Two episodes of Paleoproterozoic mafic intrusions from Liaoning province, North China Craton: Petrogenesis and tectonic implications. *Precambrian Res.* **2015**, *264*, 119–139. [CrossRef]
73. Li, S.Z.; Zhao, G.; Santosh, M.; Liu, X.; Dai, L.; Suo, Y.; Tam, P.Y.; Song, M.; Wang, P. Paleoproterozoic structural evolution of the southern segment of the Jiao-Liao-Ji Belt, North China Craton. *Precambrian Res.* **2012**, *200–203*, 59–73. [CrossRef]
74. Li, S.Z.; Zhao, G.; Wilde, S.A.; Zhang, J.; Sun, M.; Zhang, G.; Dai, L. Deformation history of the Hengshan–Wutai–Fuping Complexes: Implications for the evolution of the Trans-North China Orogen. *Gondwana Res.* **2010**, *18*, 611–631. [CrossRef]
75. Peng, C.; Xue, L.-F.; Zhu, M.; Chai, Y.; Liu, W.-Y. The location and evolution of the tectonic boundary between the Paleoproterozoic Jiao-Liao-Ji Belt and the Longgang Block, northeast China. *Precambrian Res.* **2016**, *272*, 18–38. [CrossRef]
76. Kusky, T.M.; Polat, A.; Windley, B.F.; Burke, K.C.; Dewey, J.F.; Kidd, W.S.F.; Maruyama, S.; Wang, J.P.; Deng, H.; Wang, Z.S.; et al. Insights into the tectonic evolution of the North China Craton through comparative tectonic analysis: A record of outward growth of Precambrian continents. *Earth Sci. Rev.* **2016**, *162*, 387–432. [CrossRef]
77. Xu, W.; Liu, F.L.; Liu, C.H. Petrogenesis and geochemical characteristics of the North Liaohe metabasic rocks, Jiao-Liao-Ji orogenic belt and their tectonic significance. *Yanshi Xuebao/Acta Petrol. Sin.* **2017**, *33*, 2743–2757.